Electronic Supplementary Material (ESI) for New Journal of Chemistry.

Supporting Information

Participation of Non-Aminoisobutyric Acid (Aib) Residues in the 3_{10} Helical Conformation of Aib-Rich Foldamers: A Solid State Study

Sarah J. Pike,*‡ Thomas Boddaert,‡ James Raftery,‡ Simon J. Webb†‡* Jonathan Clayden,*‡

‡School of Chemistry, University of Manchester, Oxford Road, Manchester, M13 9PL, UK.

†Manchester Institute of Biotechnology, University of Manchester, 131 Princess St., Manchester, M1 7DN, UK.

Email: s.webb@manchester.ac.uk, clayden@manchester.ac.uk

Crystallographic Details

Single crystals of **1**, **2** and **4**-**5** suitable for X-ray diffraction analysis were grown by slow evaporation of a saturated solution of chloroform. Single crystals of **3** suitable for X-ray diffraction analysis were grown by slow evaporation of a saturated solution of methanol and di-ethyl ether. Single crystals of **6** suitable for X-ray diffraction analysis were grown by slow evaporation of a saturated solution of methanol. The data was collected, reduced and solved and refined under APEX2 program suite on a Bruker Prospector with Cu radiation for Cbz-Phe-$(Aib)_4$-O^{t}Bu. For N_3-$(Aib)_4$-$GlyNH_2$, Saint crashed during data reduction but data reduced successfully with CrysAlisPro. For Cbz-L-Phe-$(Aib)_4$-Ac_6c-$(Aib)_4$-$GlyNH_2$, Cbz-L-Phe-$(Aib)_4$-NH_2, Cbz-L-Phe-$(Aib)_4$-Ac_5c-$(Aib)_4$-$GlyNH_2$, Cbz-L-Phe-$(Aib)_4$-Bip-$(Aib)_4$-$GlyNH_2$ data was collected, reduced and solved and refined under APEX1 program suite on a Bruker SMART AXS with Mo radiation. For Cbz-Phe-$(Aib)_4$-O^{t}Bu, Prospector with Cu radiation: Cbz-Phe-$(Aib)_4$-O^{t}Bu. The actual component programs for reduction, solution and refinement are Saint, SHELXS-97 and SHELXL-97. The following restraints/constraints were used: EADP and SADI for Cbz-Phe-$(Aib)_4$-O^{t}Bu, FLAT SADI ISOR and SADI for Cbz-L-Phe-$(Aib)_4$-Bip-$(Aib)_4$-$GlyNH_2$, SADI and ISOR for Cbz-L-Phe-$(Aib)_4$-Ac_5c-$(Aib)_4$-$GlyNH_2$, DANG and DFIX for Cbz-L-Phe-$(Aib)_4$-NH_2, DFIX for Cbz-L-Phe-$(Aib)_4$-Ac_6c-$(Aib)_4$-$GlyNH_2$ and non for N_3-$(Aib)_4$-$GlyNH_2$. Disorder was found in the following structures; benzyl group and chloroform molecules of Cbz-Phe-$(Aib)_4$-O^{t}Bu, phenyl groups, a water molecule and a Me_2C residue in Cbz-L-Phe-$(Aib)_4$-Ac_5c-$(Aib)_4$-$GlyNH_2$ but no disorder was found for N_3-$(Aib)_4$-$GlyNH_2$, Cbz-L-Phe-$(Aib)_4$-Bip-$(Aib)_4$-$GlyNH_2$, Cbz-L-Phe-$(Aib)_4$-NH_2or Cbz-L-Phe-$(Aib)_4$-Ac_6c-$(Aib)_4$-$GlyNH_2$. For Cbz-L-Phe-$(Aib)_4$-Ac_5c-$(Aib)_4$-$GlyNH_2$, the structure was solved by the direct methods and there are two molecules in the asymmetric unit together with some water molecules, some at partial occupancy. All non-H atoms were refined anisotropically with restraints. Most H atoms were included in calculated positions; those bonded to the water molecules could not be located.

General Experimental Section

Nuclear Magnetic Resonance (NMR) spectra were recorded on a Bruker Ultrashield 400 or 500 MHz spectrometer. ^{1}H and ^{13}C spectra were referenced relative to the solvent residual peaks and chemical shifts (δ) reported in ppm downfield of tetramethylsilane ($CDCl_3$ δ H: 7.26 ppm, δ C: 77.0 ppm). Coupling constants (J) are reported in Hertz and rounded to 0.1 Hz. Splitting patterns are abbreviated as follows: singlet (s), doublet (d), multiplet (m), septet (spt), broad (br) or some combination of these.

Low and high resolution mass spectra were recorded by staff at the University of Manchester. Electrospray (ES) spectra were recorded on a Waters Platform II and high resolution mass spectra (HRMS) were recorded on a Thermo Finnigan MAT95XP and are accurate to ± 0.001 Da. Infrared spectra were recorded on a Thermo Scientific Nicolet iS5 FTIR Spectrometer. Melting points were determined on a GallenKamp apparatus and are uncorrected. Thin layer chromatography (TLC) was performed using commercially available pre-coated plates (Macherey-Nagel alugram. Sil G/UV254) and visualized with UV light at 254 nm; phosphomolybdic acid dip was used to reveal the products. Flash column chromatography was carried out using Fluorochem Davisil 40-63u 60Å.

All reactions were conducted under a nitrogen atmosphere in oven-dried glassware unless stated otherwise. Dichloromethane was obtained by distillation over calcium hydride under a nitrogen atmosphere. All other solvents and commercially available reagents were used as received.

Procedures for the synthesis of H_2N-Aib_4O^t-Bu,[1] Cbz-L-Phe-Aib_4O^t-Bu[2] and Cbz-D-Phe-Aib_4O^t-Bu[2] have been reported previously. The following abbreviations have been used; Aib = aminoisobutyric acid, Cbz = benzyloxycarbonyl, Phe = phenylalanine, ^{t}Bu = *tert*-butyl.

Synthetic Details

CbzPheAib$_4$O^{t}Bu

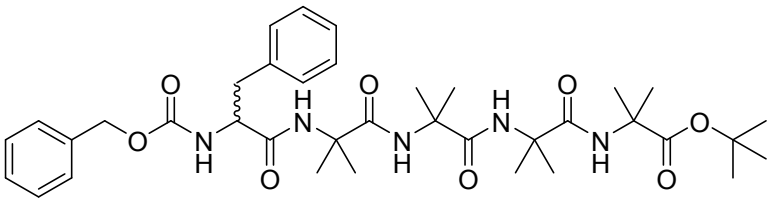

A solution of Cbz-L-PheAib$_4$O^{t}Bu (0.050 g, 0.072 mmol) in CH_2Cl_2 (3 mL) was added Cbz-D-PheAib$_4$O^{t}Bu (0.050 g, 0.072 mmol) and the reaction mixture was left stirring at ambient temperature for 5 mins. After this time, the excess solvent was removed under reduced pressure and to give a white solid. **m.p.** 248-250 ºC; ^{1}H NMR (500MHz, $CDCl_3$); δ = 7.38 – 7.27 (m, 9H, Ar*H* + N*H*), 7.18 (d, 2H, J = 6.8 Hz, Ar*H*), 7.10 (s, br, 1H, N*H*), 6.92 (s, br, 1H, N*H*), 6.13 (s, br, 1H, N*H*), 5.37 (d, 1H, J = 12.0 Hz, N*H*), 5.10 (d, A of AB, 1H, J = 12.2 Hz, C*H* of CH_2), 5.07 (d, B of AB, 1H, J = 12.2 Hz, C*H* of CH_2), 4.11 – 4.09 (m, 1H, C*H*), 3.13 (dd, 1H, J = 14.0 Hz, ^{4}J = 6.4 Hz, C*H* of CH_2), 2.99 (dd, 1H, J = 14.0 Hz, ^{4}J = 8.2 Hz, C*H* of CH_2), 1.51 (6H, s, 2 × CH_3, Aib), 1.47 (6H, s, 2 × CH_3, Aib), 1.43 (9H, s, 3 × CH_3, O^{t}Bu), 1.41 (6H, s, 2 × CH_3, Aib), 1.40 (6H, s, 2 × CH_3, Aib), 1.34 (6H, s, 2 × CH_3, Aib), 1.27 (6H, s, 2 × CH_3, Aib), ^{13}C NMR (125 MHz, $CDCl_3$); 174.1 (CO), 173.7 (CO), 173.2 (CO), 173.0 (CO), 171.0 (CO), 170.8 (CO), 135.8 (Ar), 135.7 (Ar), 129.2 (Ar), 129.0 (Ar), 128.7 (2C, Ar), 128.6 (Ar), 128.2 (2C, Ar), 127.5 (Ar), 79.9 (C), 67.6 (*C*H$_2$), 57.5 (CH$_2$), 57.0 (C), 56.9 (C), 56.7 (C), 56.1 (C), 36.7 (CH$_2$), 27.9 (CH$_3$,O^{t}Bu), 25.6 (CH$_3$, Aib), 25.4 (CH$_3$, Aib), 25.34 (CH$_3$, Aib), 25.30 (CH$_3$, Aib), 25.0 (CH$_3$, Aib), 24.8 (CH$_3$, Aib), 24.7 (CH$_3$, Aib), 24.6 (CH$_3$, Aib); **IR** 3324, 2983, 2933, 1707, 1665, 1526, 1467, 1455, 1384, 1364, 1258, 1148, 1028; **MS** (ES$^+$, MeOH): *m/z* = 695 ([M+H]$^+$, 12%), 719 ([M+Na]$^+$, 8%).

Crystal Structure Data for Cbz-L-Phe-$(Aib)_4$-NH_2

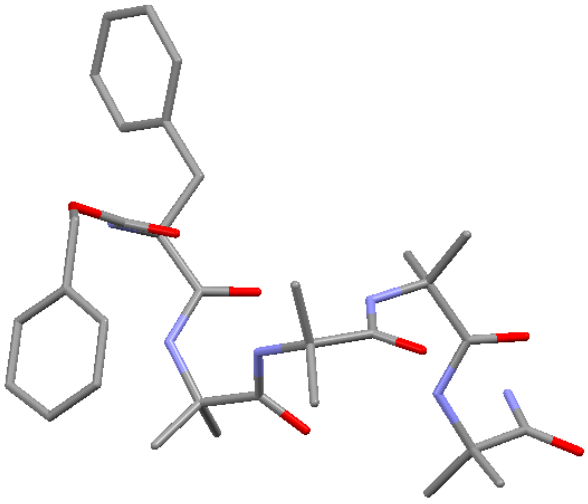

Table S1. Crystal data and structure refinement for Cbz-L-Phe-$(Aib)_4$-NH_2

Identification code	Cbz-L-Phe-$(Aib)_4$-NH_2
Empirical formula	C33 H46 N6 O7
Formula weight	638.76
Temperature	100(2) K
Wavelength	0.71073 A
Crystal system, space group	Triclinic, P1
Unit cell dimensions	a = 11.357(2) alpha = 80.846(4) b = 16.271(3) beta = 87.004(4) c = 18.895(4) gamma = 89.866(4)
Volume	3442.2(12) A^3
Z, Calculated density	4, 1.233 Mg/m^3
Absorption coefficient	0.088 mm^-1
F(000)	1368
Crystal size	0.50 x 0.40 x 0.40 mm
Theta range for data collection	1.54 to 26.40 deg.
Limiting indices	-14<=h<=14, -20<=k<=20, -22<=l<=23
Reflections collected / unique	27363 / 13809 [R(int) = 0.0658]
Completeness to theta = 26.40	97.8 %
Absorption correction	None
Refinement method	Full-matrix least-squares on F^2

Data / restraints / parameters	13809 / 41 / 1773
Goodness-of-fit on F^2	0.872
Final R indices [I>2sigma(I)]	R1 = 0.0513, wR2 = 0.0967
R indices (all data)	R1 = 0.0952, wR2 = 0.1082
Largest diff. peak and hole	0.294 and -0.180 e.A^-3

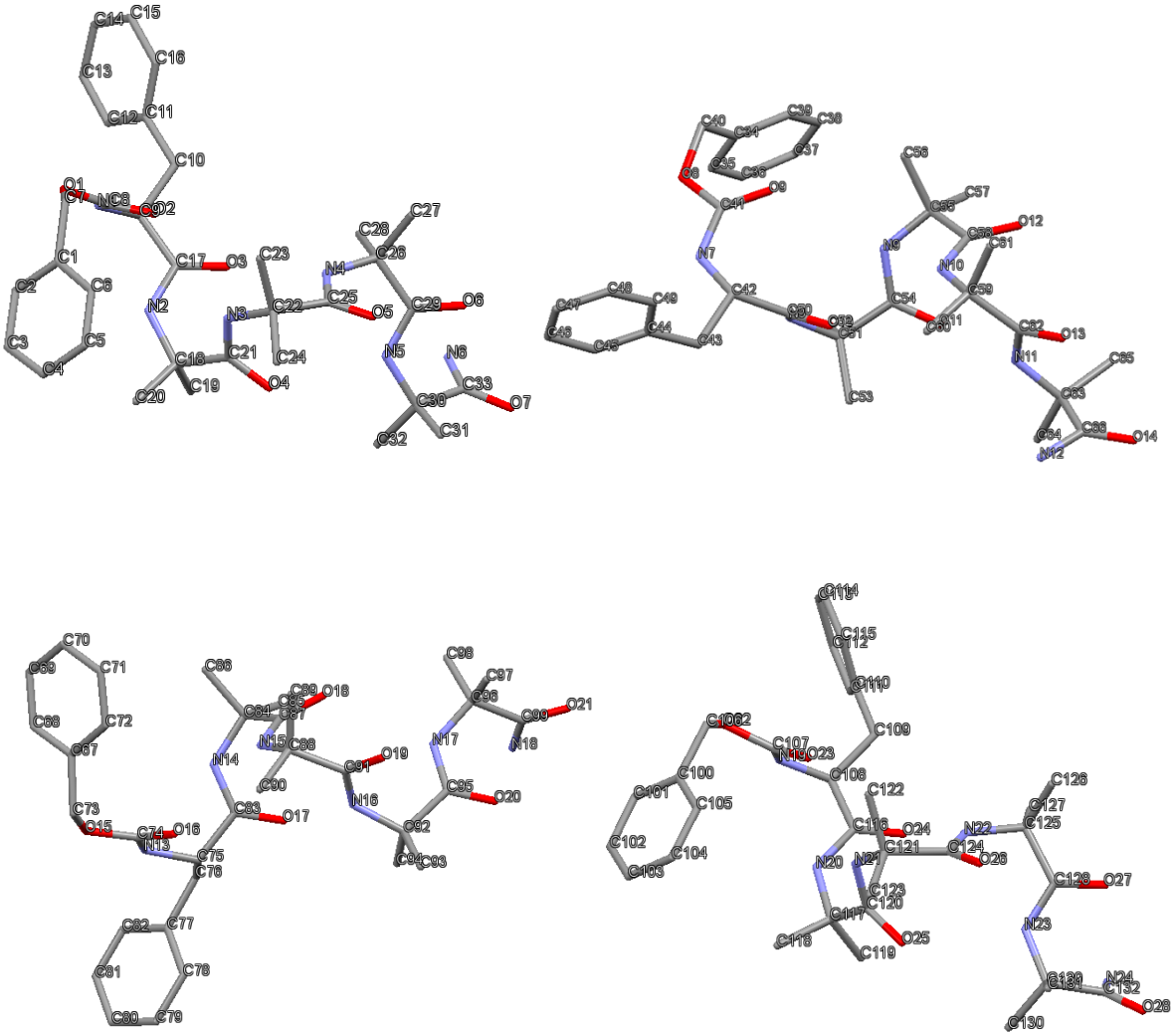

Table S2. Hydrogen bonds for Cbz-L-Phe-$(Aib)_4$-NH_2 [A and deg.].

D-H...A	d(D-H)	d(H...A)	d(D...A)	<(DHA)
N(1)-H(1N)...O(6)#1	0.88(2)	1.99(3)	2.737(5)	141(4)
N(3)-H(3N)...O(2)	0.87(2)	2.27(3)	3.075(6)	153(5)
N(4)-H(4N)...O(3)	0.88(2)	2.16(2)	3.013(6)	166(5)
N(5)-H(5N)...O(4)	0.88(2)	2.26(3)	3.108(6)	160(5)
N(6)-H(6L)...O(14)#2	0.822(19)	1.86(2)	2.681(5)	173(4)
N(7)-H(7N)...O(13)#3	0.87(2)	1.91(2)	2.762(5)	164(5)
N(9)-H(9N)...O(9)	0.86(2)	2.31(2)	3.153(6)	168(5)
N(10)-H(10N)...O(10)	0.85(2)	2.18(3)	2.961(5)	152(5)
N(11)-H(11N)...N(10)	0.85(2)	2.28(5)	2.793(7)	118(4)
N(11)-H(11N)...O(11)	0.85(2)	2.31(3)	3.110(6)	155(5)
N(12)-H(12L)...O(14)	0.779(19)	1.78(5)	2.260(5)	119(5)
N(12)-H(12M)...O(7)#4	0.808(18)	1.86(2)	2.645(6)	165(4)
N(13)-H(13N)...O(20)#1	0.847(19)	1.95(2)	2.773(5)	163(5)
N(15)-H(15N)...O(16)	0.87(2)	2.40(3)	3.123(6)	141(4)
N(16)-H(16N)...O(17)	0.87(2)	2.20(3)	2.952(6)	144(4)
N(16)-H(16N)...N(15)	0.87(2)	2.32(5)	2.763(6)	111(4)
N(17)-H(17N)...O(18)	0.889(19)	2.19(3)	3.029(5)	157(4)
N(18)-H(18L)...O(11)#3	0.821(19)	1.90(2)	2.708(5)	168(4)
N(19)-H(19N)...O(27)#3	0.86(2)	1.94(3)	2.736(5)	155(5)

N(20)-H(20N)...O(28)#3	0.866(19)	2.52(4)	3.177(5)	133(4)
N(21)-H(21N)...O(23)	0.87(2)	2.12(2)	2.996(6)	179(5)
N(22)-H(22N)...O(24)	0.865(19)	2.14(2)	3.002(5)	173(4)
N(23)-H(23N)...O(25)	0.89(2)	2.13(2)	2.996(5)	163(4)
N(24)-H(24L)...O(4)#5	0.807(19)	1.91(3)	2.679(5)	159(4)
N(24)-H(24M)...O(27)	0.842(17)	2.62(3)	3.011(5)	110(2)

Torsion Angles for Cbz-L-Phe-$(Aib)_4$-NH_2.

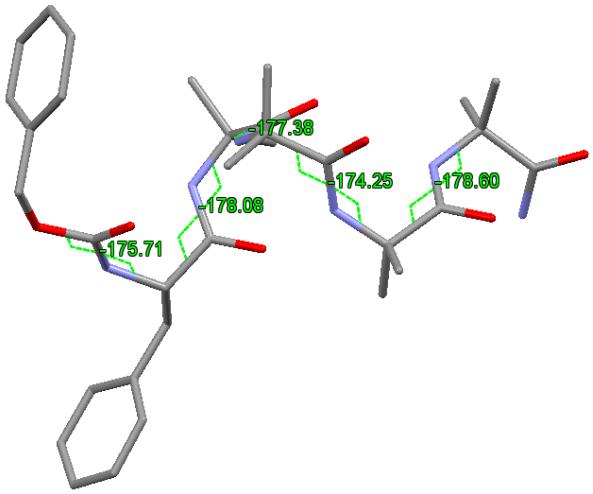

Figure S1. Highlighting the ω torsion angles for one molecule in the unit cell of Cbz-L-Phe-$(Aib)_4$-NH_2.

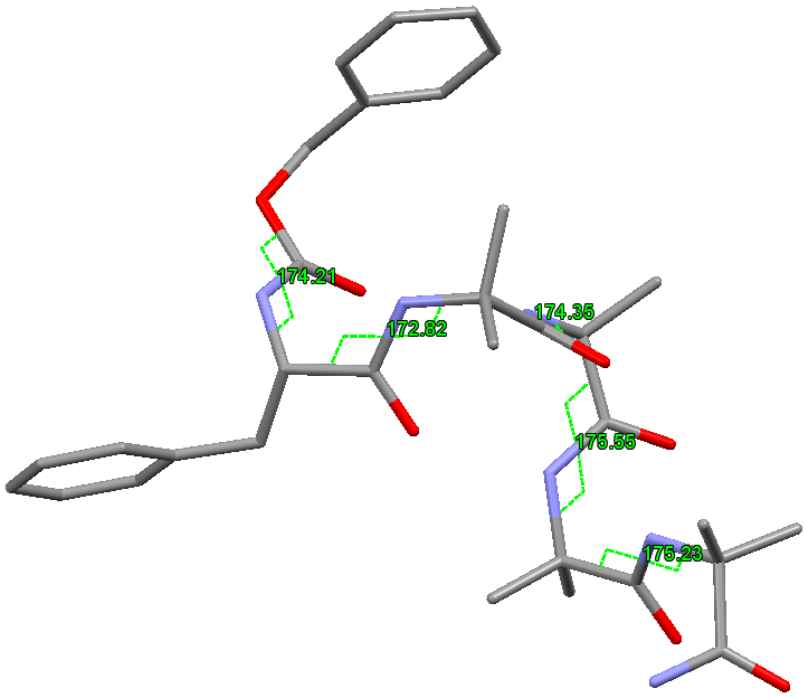

Figure S2. Highlighting the ω torsion angles for one molecule in the unit cell of Cbz-L-Phe-$(Aib)_4$-NH_2

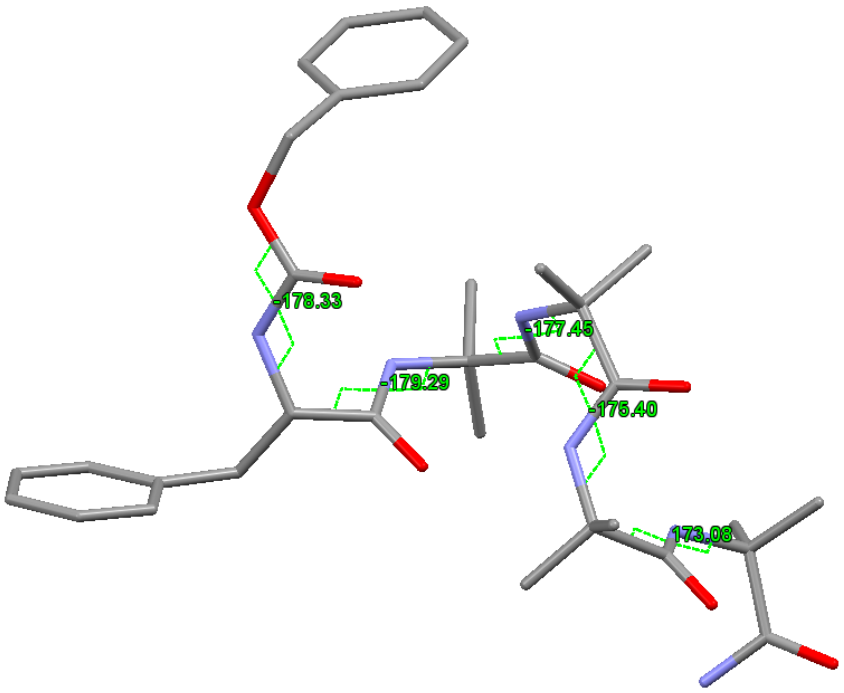

Figure S3. Highlighting the ω torsion angles for one molecule in the unit cell of Cbz-L-Phe-$(Aib)_4$-NH_2.

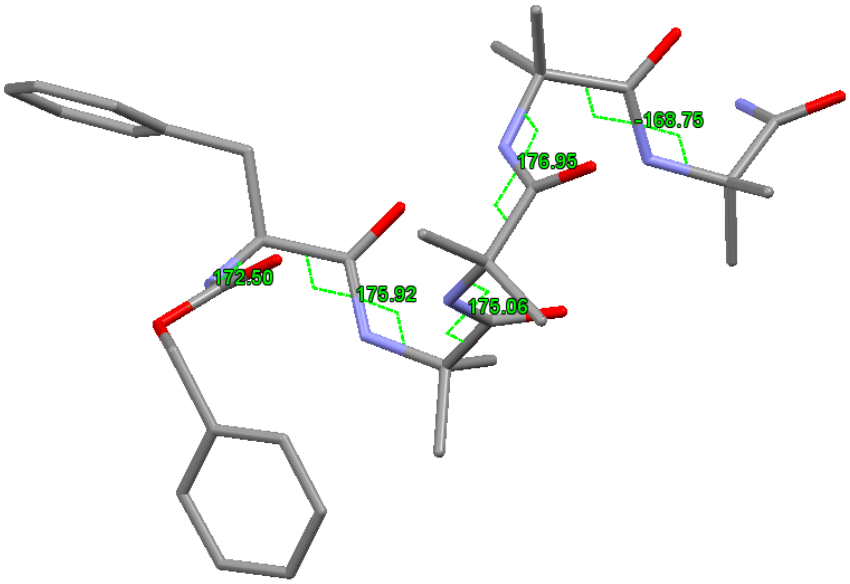

Figure S4. Highlighting the ω torsion angles for one molecule in the unit cell of Cbz-L-Phe-$(Aib)_4$-NH_2.

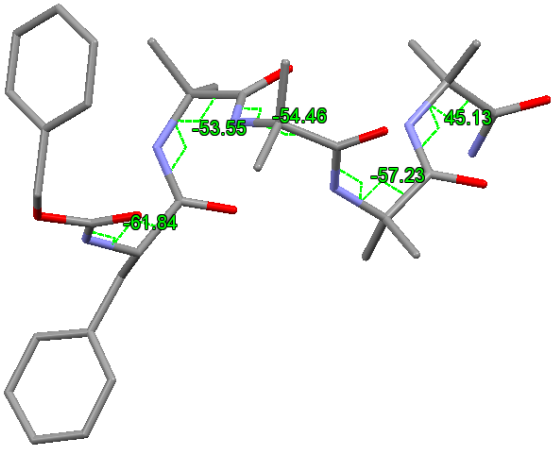

Figure S5. Highlighting the ϕ torsion angles for one molecule in the unit cell of Cbz-L-Phe-$(Aib)_4$-NH_2.

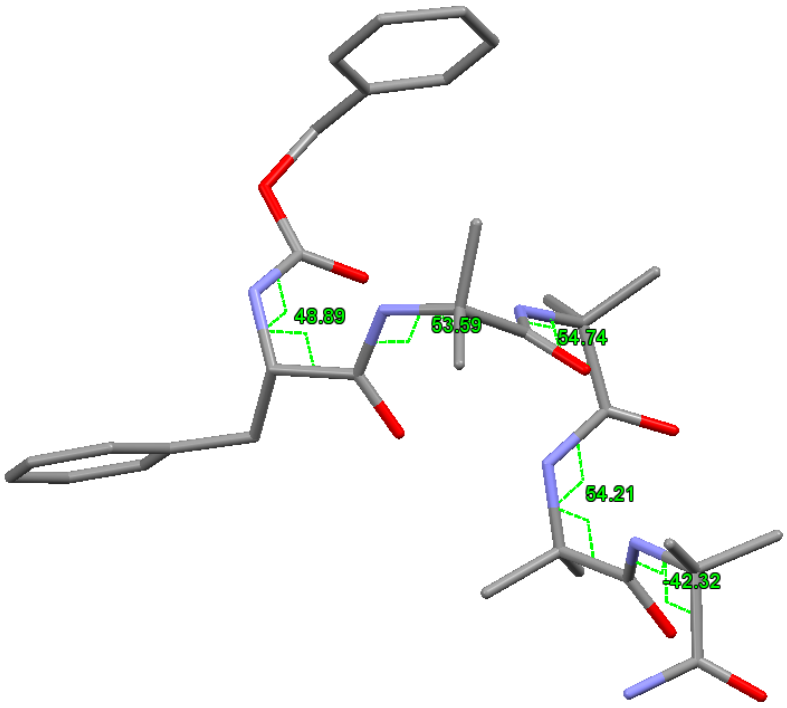

Figure S6. Highlighting the ϕ torsion angles for one molecule in the unit cell of Cbz-L-Phe-$(Aib)_4$-NH_2.

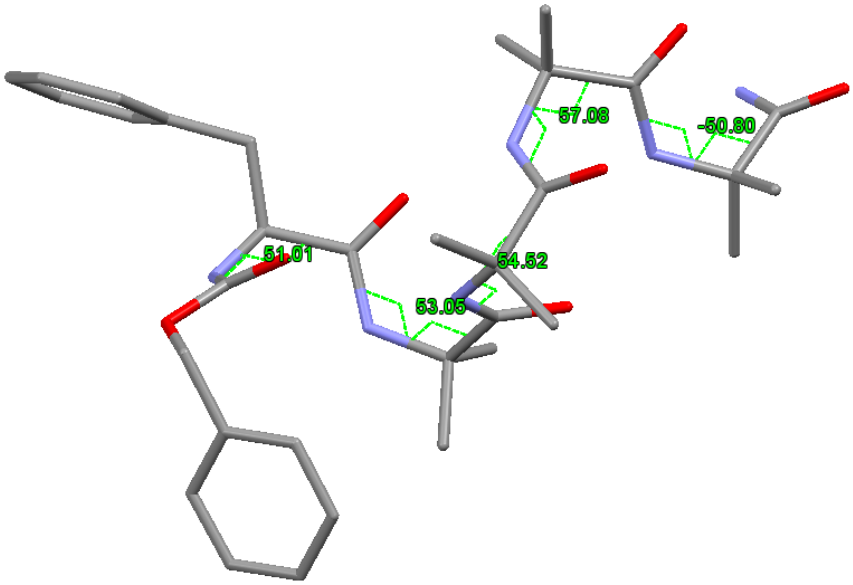

Figure S7. Highlighting the ϕ torsion angles for one molecule in the unit cell of Cbz-L-Phe-$(Aib)_4$-NH_2.

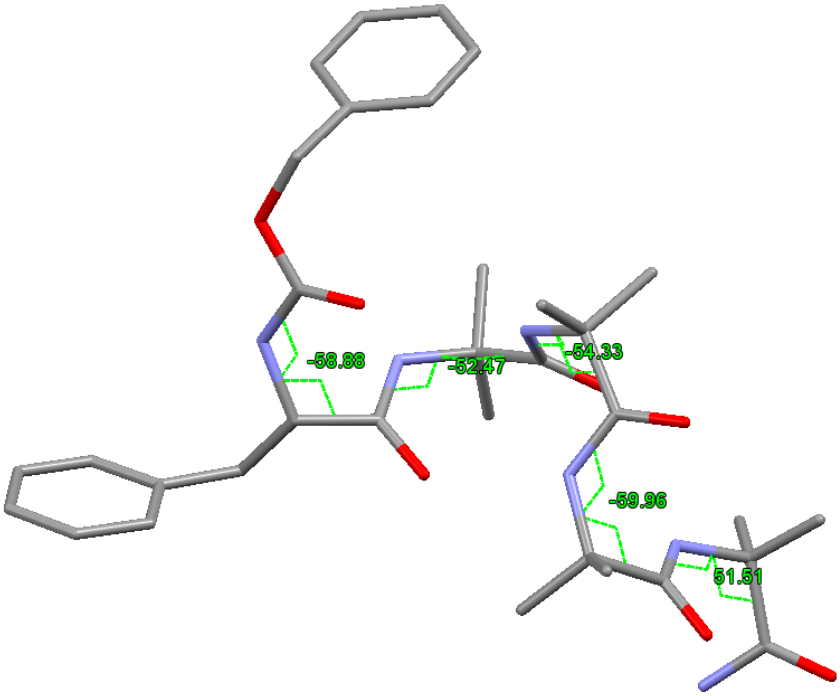

Figure S8. Highlighting the ϕ torsion angles for one molecule in the unit cell of Cbz-L-Phe-$(Aib)_4$-NH_2.

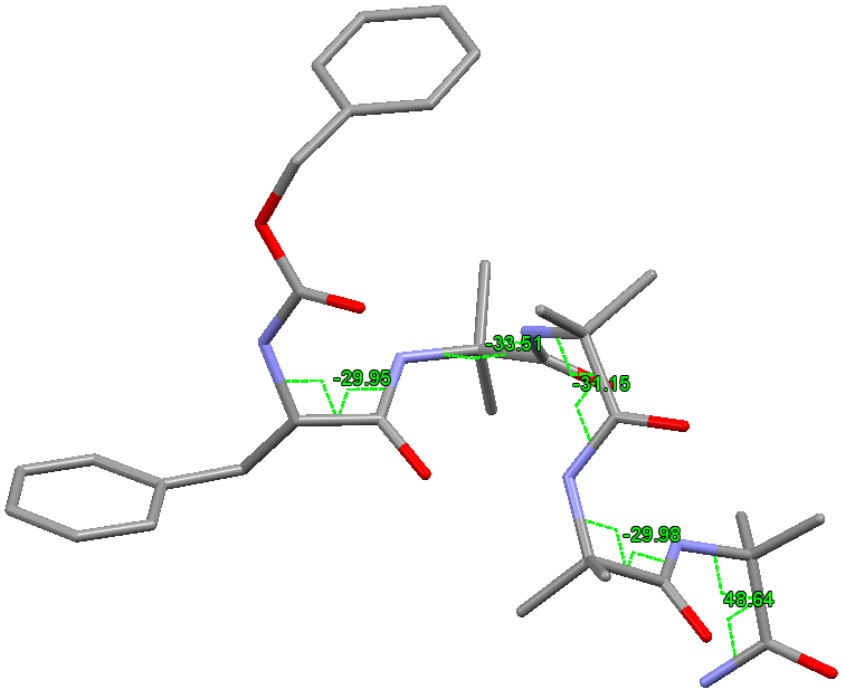

Figure S9. Highlighting the ψ torsion angles for one molecule in the unit cell of Cbz-L-Phe-$(Aib)_4$-NH_2.

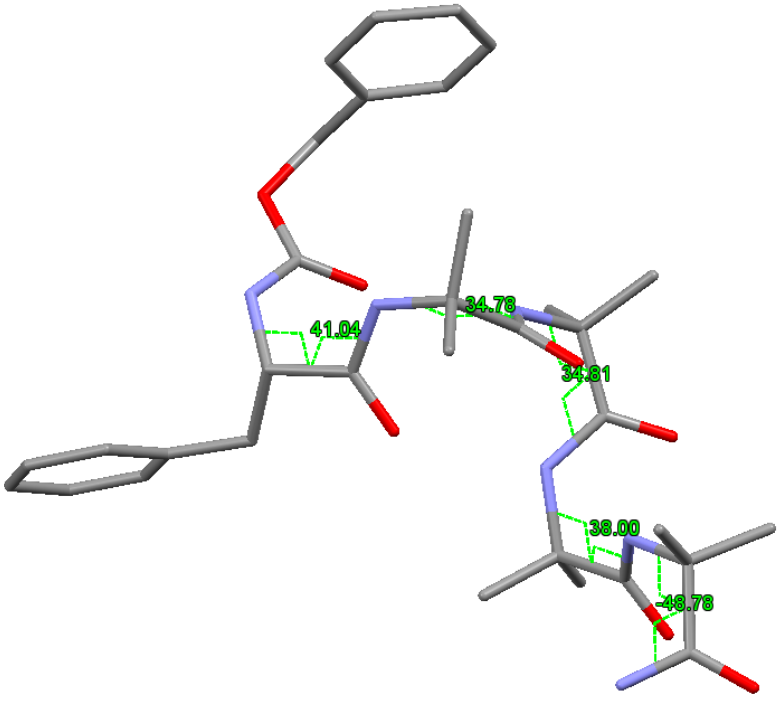

Figure S10. Highlighting the ψ torsion angles for one molecule in the unit cell of Cbz-L-Phe-$(Aib)_4$-NH_2.

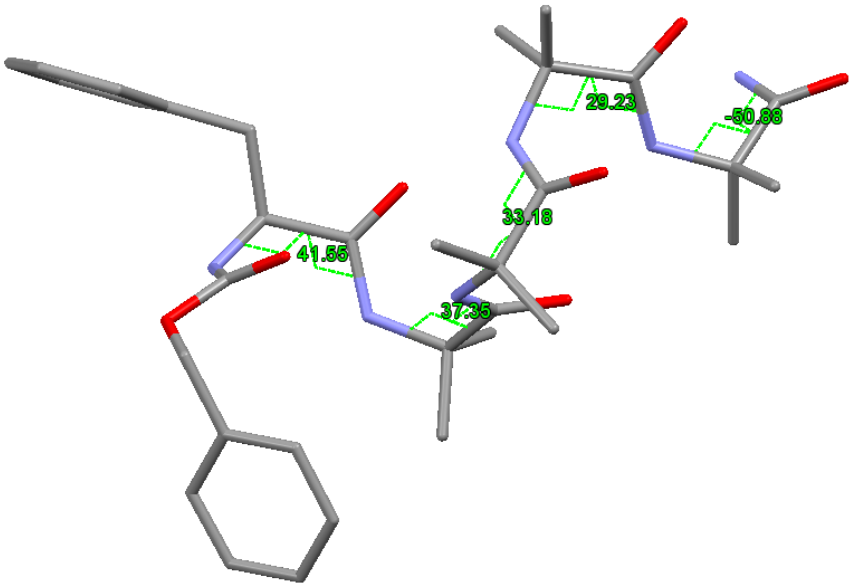

Figure S11. Highlighting the ψ torsion angles for one molecule in the unit cell of Cbz-L-Phe-$(Aib)_4$-NH_2.

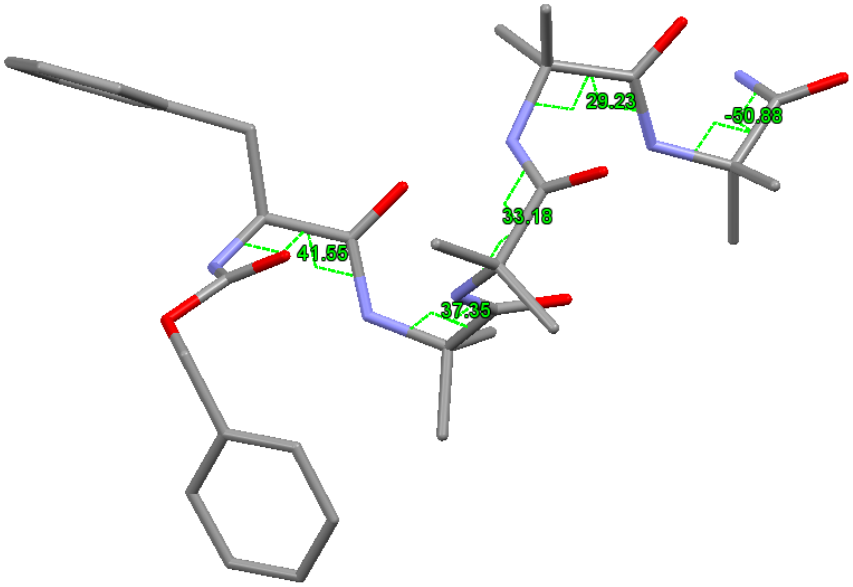

Figure S12. Highlighting the ψ torsion angles for one molecule in the unit cell of Cbz-L-Phe-$(Aib)_4$-NH_2.

Intramolecular Hydrogen-bonding interactions in Cbz-L-Phe-$(Aib)_4$-NH_2.

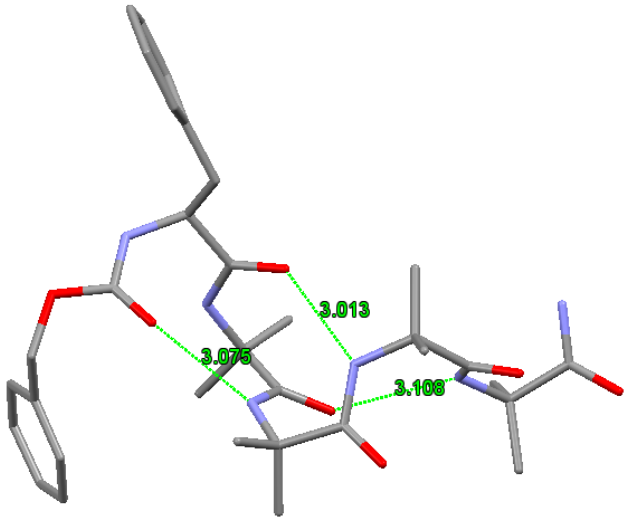

Figure S13. Intramolecular hydrogen bonding interactions present in one molecule of Cbz-L-Phe-$(Aib)_4$-NH_2 found in the unit cell.

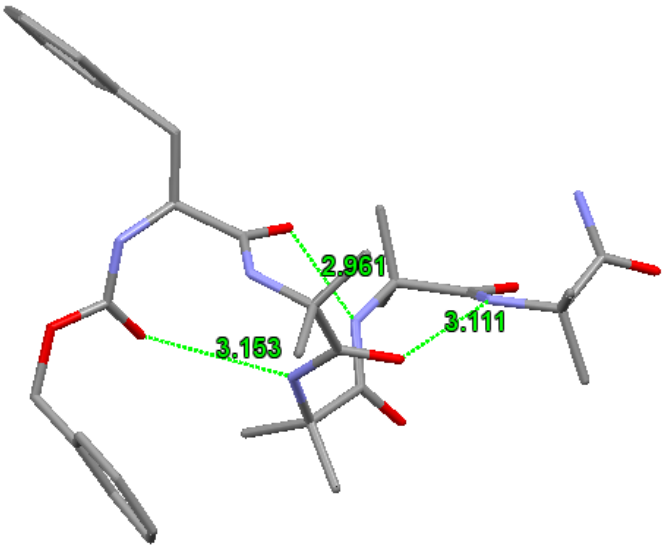

Figure S14. Intramolecular hydrogen bonding interactions present in one molecule of Cbz-L-Phe-$(Aib)_4$-NH_2 found in the unit cell.

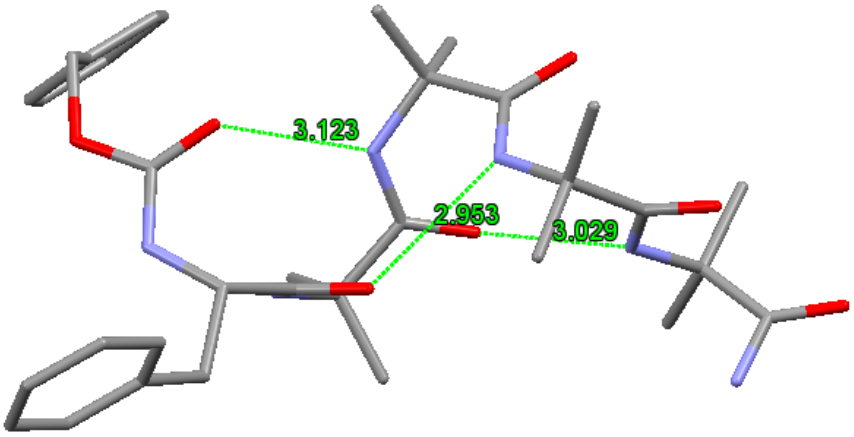

Figure S15. Intramolecular hydrogen bonding interactions present in one molecule of Cbz-L-Phe-$(Aib)_4$-NH_2 found in the unit cell.

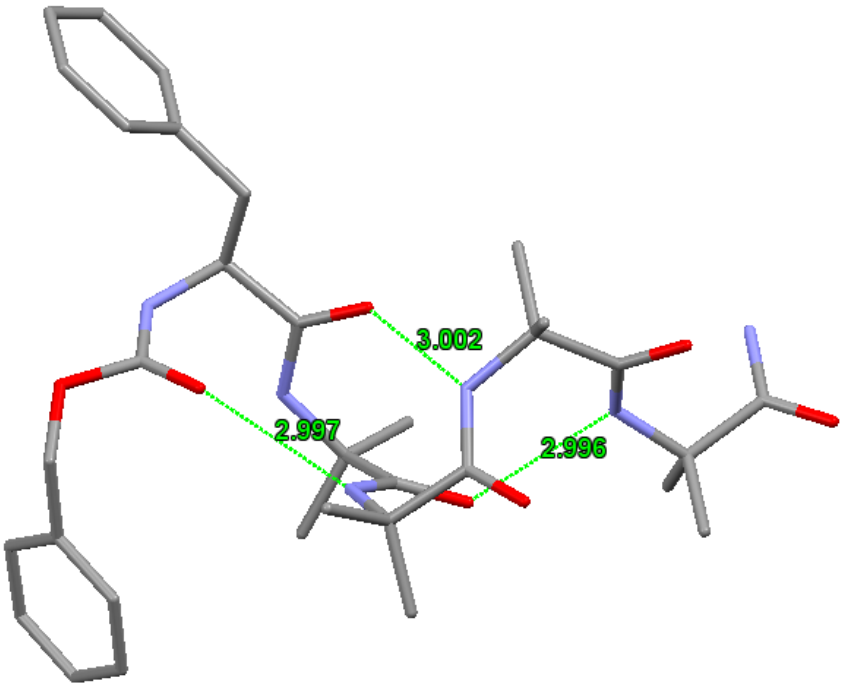

Figure S16. Intramolecular hydrogen bonding interactions present in one molecule of Cbz-L-Phe-$(Aib)_4$-NH_2 found in the unit cell.

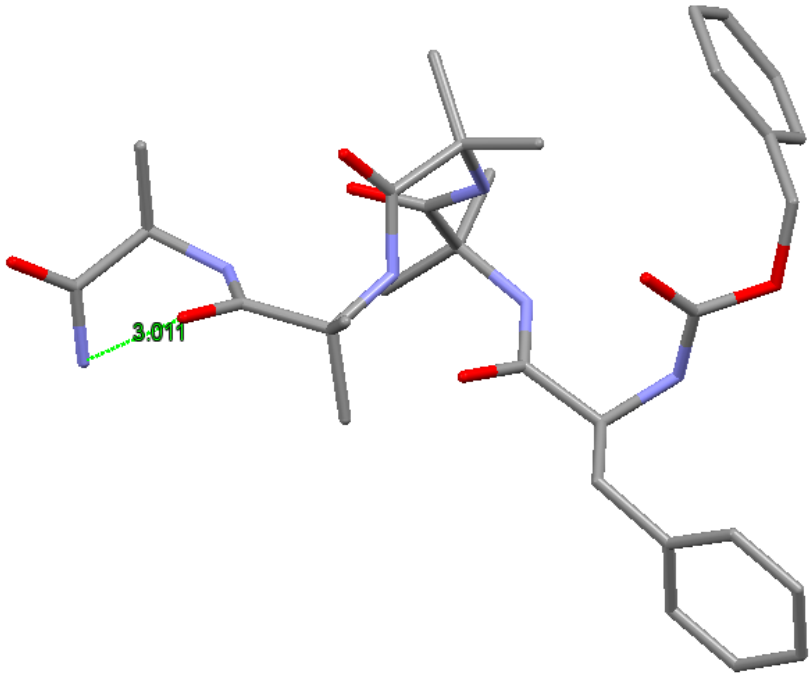

Figure S17 Intramolecular hydrogen bonding interaction present in one molecules of Cbz-L-Phe-$(Aib)_4$-NH_2 involving the C-terminal $AibNH_2$ residue which does not conform to the expected 3_{10} hydrogen-bonding pattern.

Intermolecular Hydrogen-bonding interactions in Cbz-L-Phe-$(Aib)_4$-NH_2.

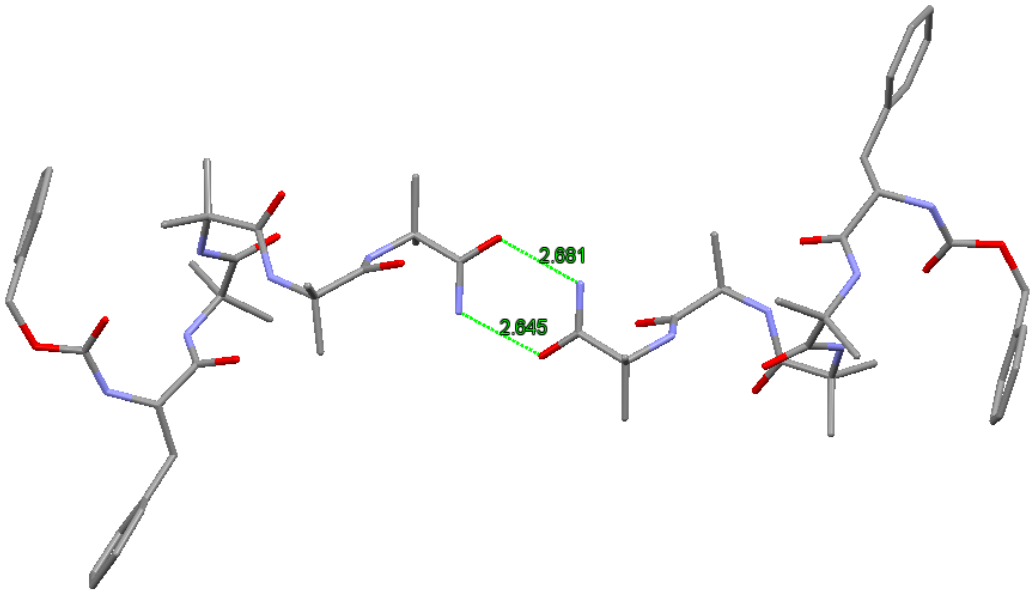

Figure S18. Intermolecular hydrogen bonding interactions present between two molecules of Cbz-L-Phe-$(Aib)_4$-NH_2 involving the C-terminal $AibNH_2$ residue.

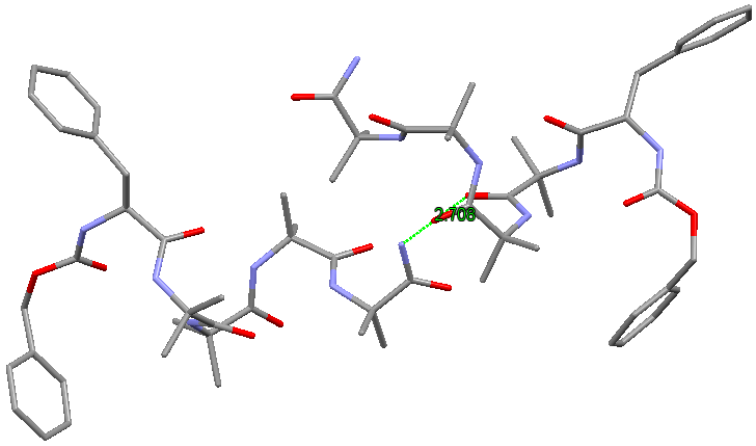

Figure S19. Intermolecular hydrogen bonding interactions present between two molecules of Cbz-L-Phe-$(Aib)_4$-NH_2 involving the C-terminal AibNH_2 residue.

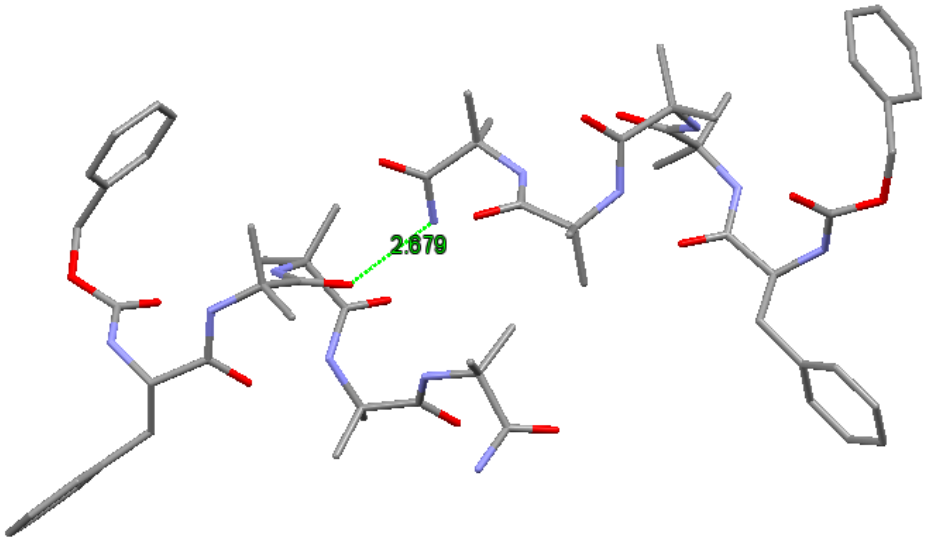

Figure S20. Intermolecular hydrogen bonding interactions present between two molecules of Cbz-L-Phe-$(Aib)_4$-NH_2 involving the C-terminal AibNH_2 residue.

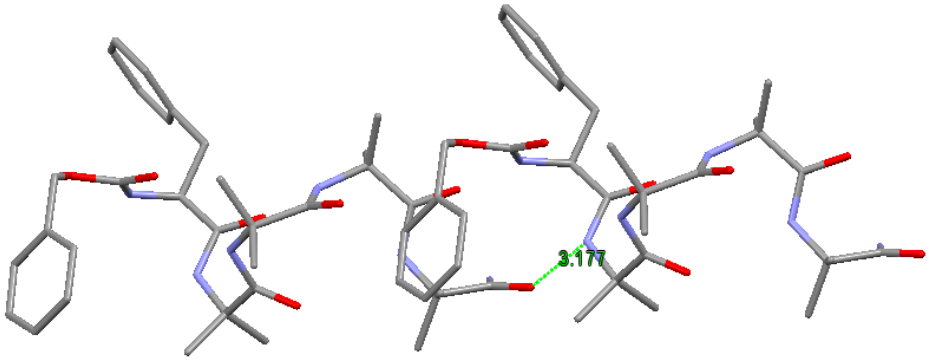

Figure S21. Intermolecular hydrogen bonding interactions present between two molecules of Cbz-L-Phe-$(Aib)_4$-NH_2 involving the C-terminal AibNH_2 residue.

Intermolecular π-π stacking interactions in Cbz-L-Phe-$(Aib)_4$-NH_2.

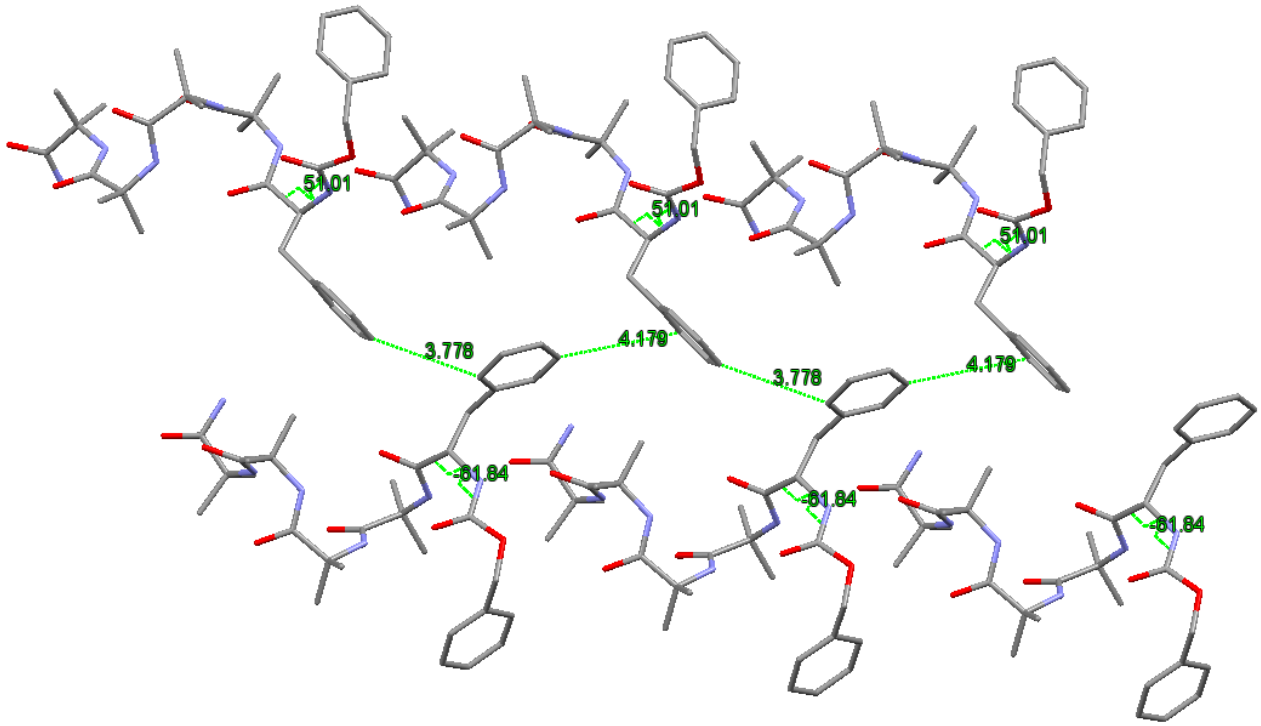

Figure S22. Intermolecular π-π stacking interactions present between two adjacent molecules of Cbz-L-Phe-$(Aib)_4$-NH_2 of opposing screw-sense.

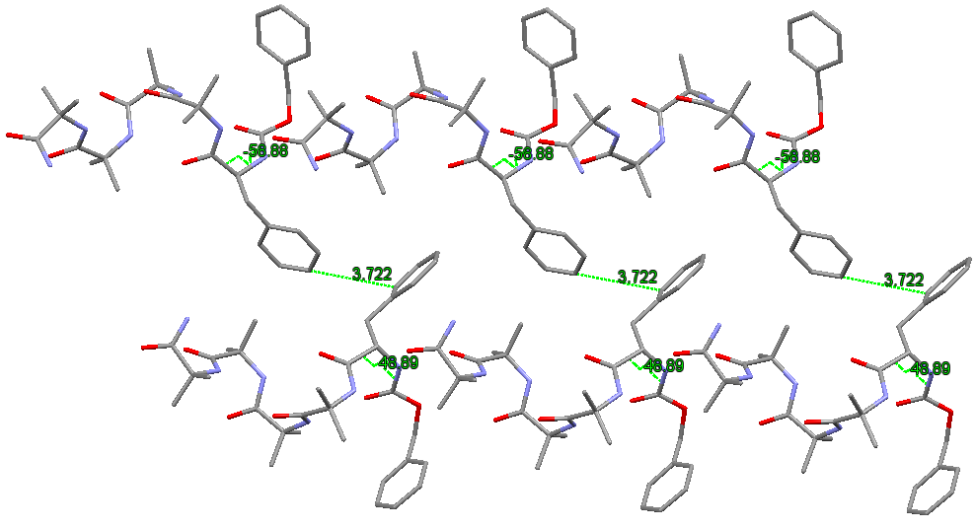

Figure S23. Intermolecular π-π stacking interactions present between two adjacent molecules of Cbz-L-Phe-$(Aib)_4$-NH_2 of opposing screw-sense.

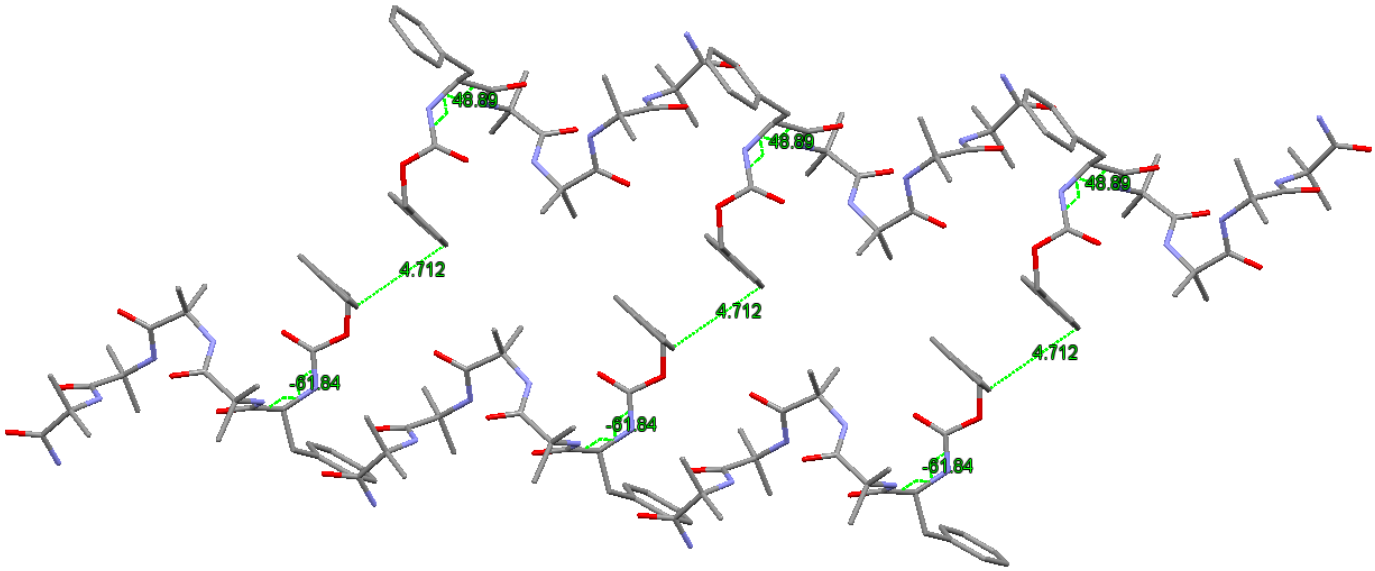

Figure S24. Intermolecular π-π stacking interactions present between two adjacent molecules of Cbz-L-Phe-$(Aib)_4$-NH_2 of opposing screw-sense.

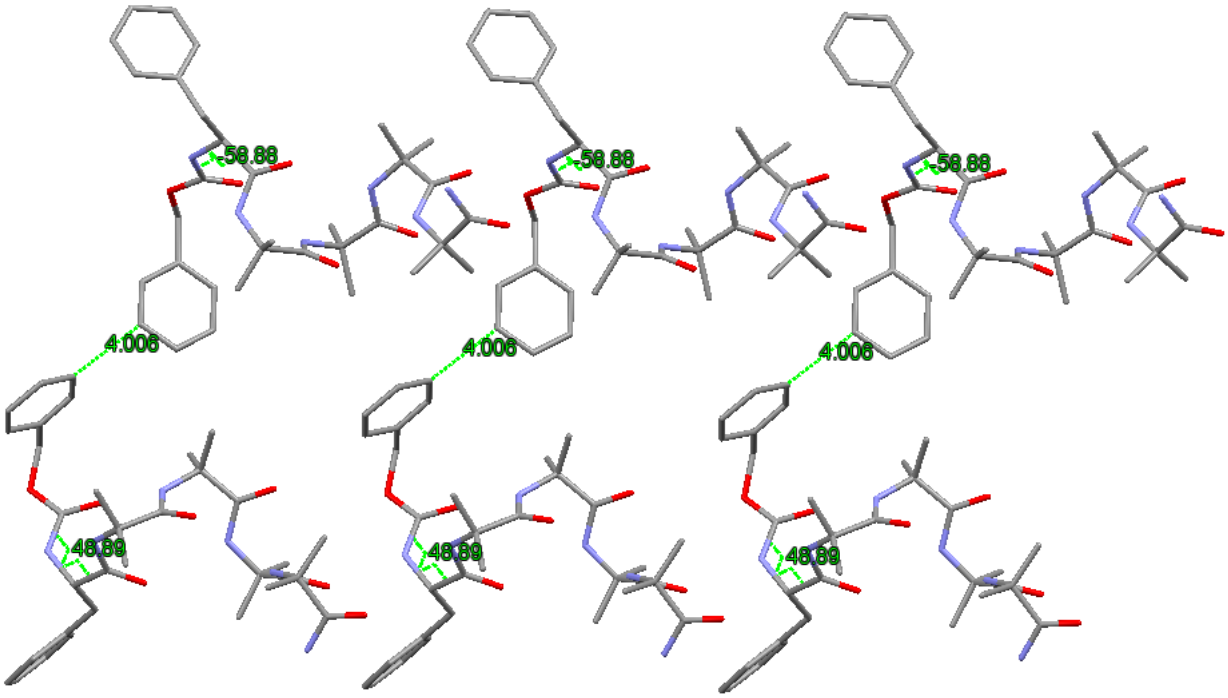

Figure S25. Intermolecular π-π stacking interactions present between two adjacent molecules of Cbz-L-Phe-$(Aib)_4$-NH_2 of opposing screw-sense.

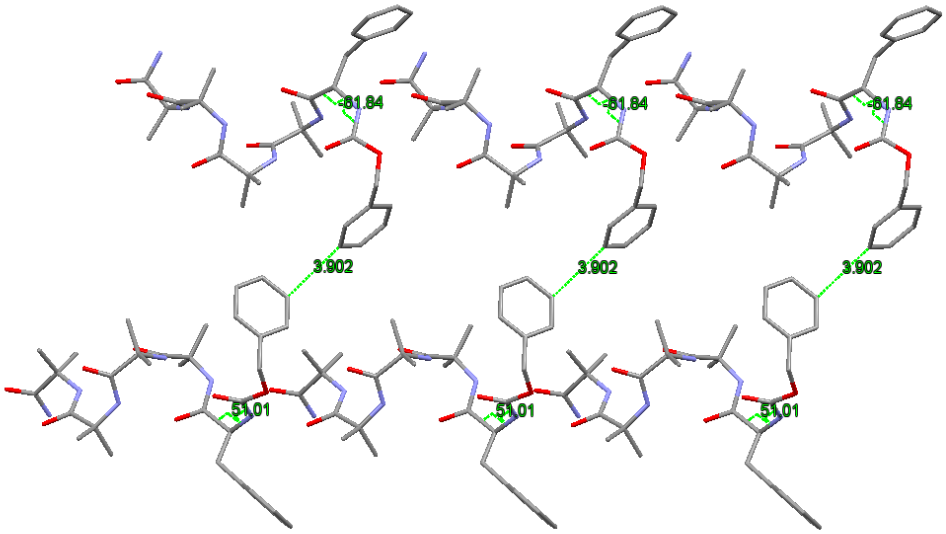

Figure S26. Intermolecular π-π stacking interactions present between two adjacent molecules of Cbz-L-Phe-$(Aib)_4$-NH_2 of opposing screw-sense.

Crystal Structure Data for Cbz-Phe-(Aib)$_4$-O*t*Bu

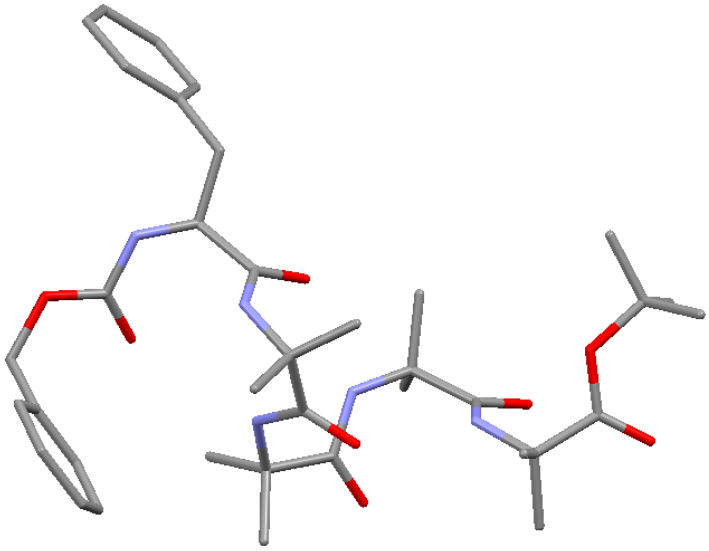

Table S3. Crystal data and structure refinement for Cbz-Phe-(Aib)$_4$-O^{t}Bu.

Identification code	Cbz-Phe(Aib)$_4$-O^{t}Bu.	
Empirical formula	C39 H55 Cl6 N5 O8	
Formula weight	934.58	
Temperature	100(2) K	
Wavelength	1.54178 Å	
Crystal system	Triclinic	
Space group	P-1	
Unit cell dimensions	a = 11.3070(4) Å	α= 70.683(2)°.
	b = 13.8002(4) Å	β= 73.734(2)°.
	c = 17.3410(5) Å	γ = 71.237(2)°.
Volume	2371.72(13) Å^3	
Z	2	
Density (calculated)	1.309 Mg/m^3	
Absorption coefficient	3.734 mm^{-1}	
F(000)	980	
Crystal size	0.29 x 0.17 x 0.08 mm^3	
Theta range for data collection	2.75 to 69.95°.	
Index ranges	-13<=h<=12, -16<=k<=16, -21<=l<=20	
Reflections collected	18687	
Independent reflections	8514 [R(int) = 0.0380]	
Completeness to theta = 67.00°	95.7 %	
Absorption correction	Semi-empirical from equivalents	
Max. and min. transmission	0.7544 and 0.497525	
Refinement method	Full-matrix least-squares on F^2	

Data / restraints / parameters	8514 / 10 / 554
Goodness-of-fit on F^2	1.070
Final R indices [I>2sigma(I)]	R1 = 0.0659, wR2 = 0.1562
R indices (all data)	R1 = 0.0815, wR2 = 0.1683
Largest diff. peak and hole	1.111 and -0.835 e.Å^{-3}

Table S4. Torsion angles [°] for Cbz-Phe-$(Aib)_4$-O^{t}Bu.

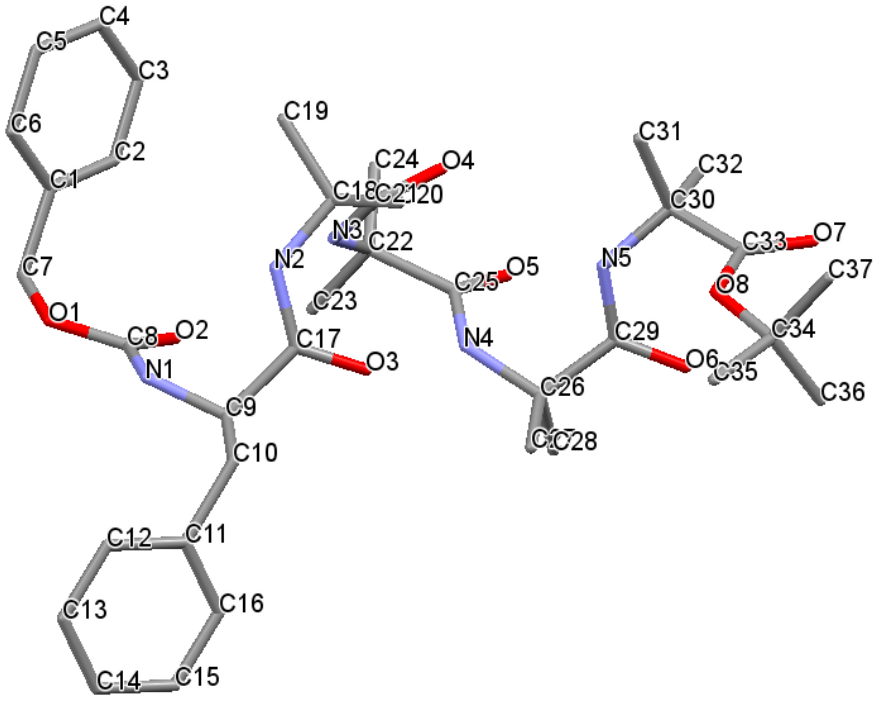

C(6)-C(1)-C(2)-C(3)	0.1(5)
C(7)-C(1)-C(2)-C(3)	-178.5(3)
C(1)-C(2)-C(3)-C(4)	-0.6(6)
C(2)-C(3)-C(4)-C(5)	0.9(6)
C(3)-C(4)-C(5)-C(6)	-0.7(6)
C(4)-C(5)-C(6)-C(1)	0.2(6)
C(2)-C(1)-C(6)-C(5)	0.1(5)
C(7)-C(1)-C(6)-C(5)	178.7(3)
C(2)-C(1)-C(7)-O(1)	-106.5(4)
C(6)-C(1)-C(7)-O(1)	75.0(4)
N(1)-C(9)-C(10)-C(11)	-75.5(4)
C(17)-C(9)-C(10)-C(11)	165.5(3)
C(9)-C(10)-C(11)-C(12)	97.2(4)

C(9)-C(10)-C(11)-C(16)	-80.5(4)
C(16)-C(11)-C(12)-C(13)	0.0
C(10)-C(11)-C(12)-C(13)	-177.7(4)
C(11)-C(12)-C(13)-C(14)	0.0
C(12)-C(13)-C(14)-C(15)	0.0
C(13)-C(14)-C(15)-C(16)	0.0
C(14)-C(15)-C(16)-C(11)	0.0
C(12)-C(11)-C(16)-C(15)	0.0
C(10)-C(11)-C(16)-C(15)	177.7(4)
C(17)-C(9S)-C(10S)-C(11S)	-173.7(8)
N(1)-C(9S)-C(10S)-C(11S)	72.0(10)
C(9S)-C(10S)-C(11S)-C(12S)	-5.6(12)
C(9S)-C(10S)-C(11S)-C(16S)	179.4(8)
C(16S)-C(11S)-C(12S)-C(13S)	0.0
C(10S)-C(11S)-C(12S)-C(13S)	-174.9(11)
C(11S)-C(12S)-C(13S)-C(14S)	0.0
C(12S)-C(13S)-C(14S)-C(15S)	0.0
C(13S)-C(14S)-C(15S)-C(16S)	0.0
C(14S)-C(15S)-C(16S)-C(11S)	0.0
C(12S)-C(11S)-C(16S)-C(15S)	0.0
C(10S)-C(11S)-C(16S)-C(15S)	175.2(10)
C(10S)-C(9S)-C(17)-O(3)	27.1(10)
N(1)-C(9S)-C(17)-O(3)	140.1(5)
C(10S)-C(9S)-C(17)-N(2)	-170.6(6)
N(1)-C(9S)-C(17)-N(2)	-57.6(8)
C(10S)-C(9S)-C(17)-C(9)	-48.5(10)
N(1)-C(9S)-C(17)-C(9)	64.6(10)
N(1)-C(9)-C(17)-O(3)	161.3(3)
C(10)-C(9)-C(17)-O(3)	-80.5(4)
N(1)-C(9)-C(17)-N(2)	-12.7(5)
C(10)-C(9)-C(17)-N(2)	105.6(4)
N(1)-C(9)-C(17)-C(9S)	-80.0(11)
C(10)-C(9)-C(17)-C(9S)	38.2(10)
N(2)-C(18)-C(21)-O(4)	155.8(3)
C(20)-C(18)-C(21)-O(4)	33.1(4)
C(19)-C(18)-C(21)-O(4)	-87.7(3)
N(2)-C(18)-C(21)-N(3)	-25.2(4)
C(20)-C(18)-C(21)-N(3)	-147.9(3)

C(19)-C(18)-C(21)-N(3)	91.3(3)
N(3)-C(22)-C(25)-O(5)	150.1(3)
C(24)-C(22)-C(25)-O(5)	26.5(4)
C(23)-C(22)-C(25)-O(5)	-93.7(3)
N(3)-C(22)-C(25)-N(4)	-33.7(3)
C(24)-C(22)-C(25)-N(4)	-157.2(2)
C(23)-C(22)-C(25)-N(4)	82.5(3)
N(4)-C(26)-C(29)-O(6)	160.8(3)
C(28)-C(26)-C(29)-O(6)	37.5(4)
C(27)-C(26)-C(29)-O(6)	-82.0(3)
N(4)-C(26)-C(29)-N(5)	-25.3(4)
C(28)-C(26)-C(29)-N(5)	-148.6(3)
C(27)-C(26)-C(29)-N(5)	91.9(3)
N(5)-C(30)-C(33)-O(7)	-137.3(3)
C(32)-C(30)-C(33)-O(7)	-15.0(4)
C(31)-C(30)-C(33)-O(7)	105.8(3)
N(5)-C(30)-C(33)-O(8)	48.0(3)
C(32)-C(30)-C(33)-O(8)	170.3(2)
C(31)-C(30)-C(33)-O(8)	-69.0(3)
O(2)-C(8)-N(1)-C(9)	8.3(5)
O(1)-C(8)-N(1)-C(9)	-172.6(3)
O(2)-C(8)-N(1)-C(9S)	-13.1(8)
O(1)-C(8)-N(1)-C(9S)	166.0(6)
C(10)-C(9)-N(1)-C(8)	170.8(3)
C(17)-C(9)-N(1)-C(8)	-71.9(4)
C(10)-C(9)-N(1)-C(9S)	-50.3(10)
C(17)-C(9)-N(1)-C(9S)	67.0(11)
C(17)-C(9S)-N(1)-C(8)	-24.8(10)
C(10S)-C(9S)-N(1)-C(8)	83.7(8)
C(17)-C(9S)-N(1)-C(9)	-78.0(11)
C(10S)-C(9S)-N(1)-C(9)	30.6(8)
O(3)-C(17)-N(2)-C(18)	-1.4(5)
C(9S)-C(17)-N(2)-C(18)	-164.5(5)
C(9)-C(17)-N(2)-C(18)	172.2(3)
C(20)-C(18)-N(2)-C(17)	67.4(4)
C(19)-C(18)-N(2)-C(17)	-171.9(3)
C(21)-C(18)-N(2)-C(17)	-54.9(4)
O(4)-C(21)-N(3)-C(22)	-5.0(4)

C(18)-C(21)-N(3)-C(22)	176.0(3)
C(24)-C(22)-N(3)-C(21)	70.3(3)
C(23)-C(22)-N(3)-C(21)	-168.3(3)
C(25)-C(22)-N(3)-C(21)	-52.5(3)
O(5)-C(25)-N(4)-C(26)	1.2(4)
C(22)-C(25)-N(4)-C(26)	-175.0(2)
C(28)-C(26)-N(4)-C(25)	61.5(3)
C(27)-C(26)-N(4)-C(25)	-177.3(2)
C(29)-C(26)-N(4)-C(25)	-61.4(3)
O(6)-C(29)-N(5)-C(30)	-8.5(4)
C(26)-C(29)-N(5)-C(30)	177.6(2)
C(32)-C(30)-N(5)-C(29)	-72.9(3)
C(33)-C(30)-N(5)-C(29)	49.7(4)
C(31)-C(30)-N(5)-C(29)	166.7(3)
O(2)-C(8)-O(1)-C(7)	6.0(5)
N(1)-C(8)-O(1)-C(7)	-173.1(3)
C(1)-C(7)-O(1)-C(8)	78.6(4)
O(7)-C(33)-O(8)-C(34)	4.3(5)
C(30)-C(33)-O(8)-C(34)	178.9(2)
C(35)-C(34)-O(8)-C(33)	175.7(3)
C(36)-C(34)-O(8)-C(33)	57.3(4)
C(37)-C(34)-O(8)-C(33)	-66.4(4)

Table S5. Hydrogen bonds for Cbz-Phe-$(Aib)_4$-O^{t}Bu [Å and °].

D-H...A	d(D-H)	d(H...A)	d(D...A)	<(DHA)
N(5)-H(5A)...O(4)	0.88	2.24	3.058(3)	153.9
N(1)-H(1)...O(6)#1	0.88	1.95	2.801(4)	163.4
N(3)-H(3A)...O(2)	0.88	2.21	3.054(3)	161.7
N(4)-H(4A)...O(3)	0.88	2.04	2.889(3)	160.6

Torsion Angles for Cbz-Phe-$(Aib)_4$-O^{t}Bu

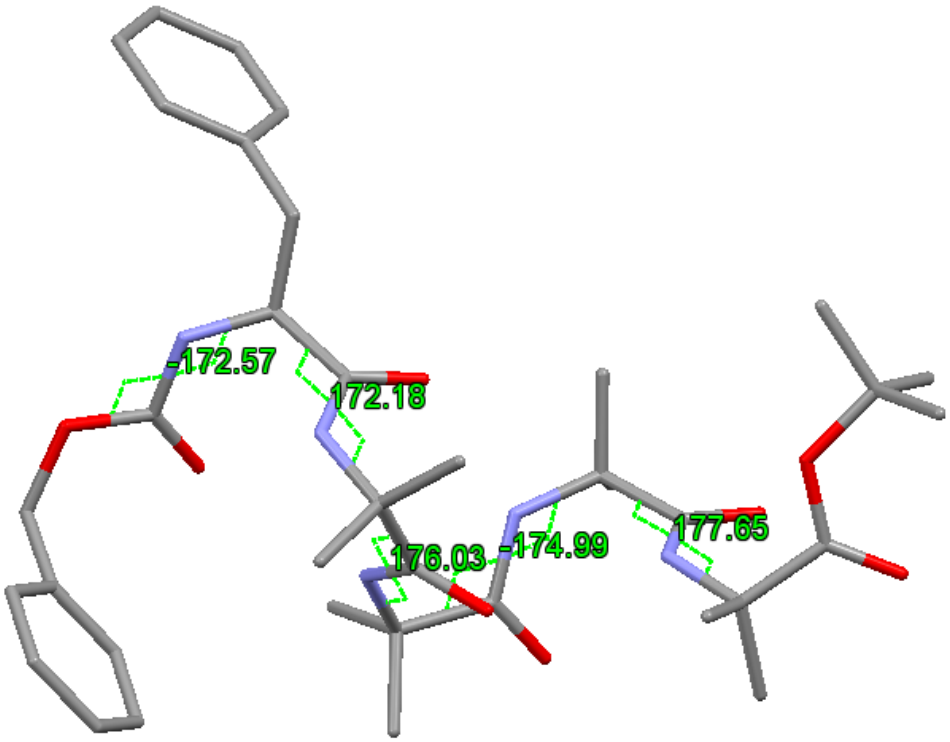

Figure S27. Highlighting the ω torsion angles for one molecule in the unit cell for Cbz-Phe-$(Aib)_4$-O^{t}Bu.

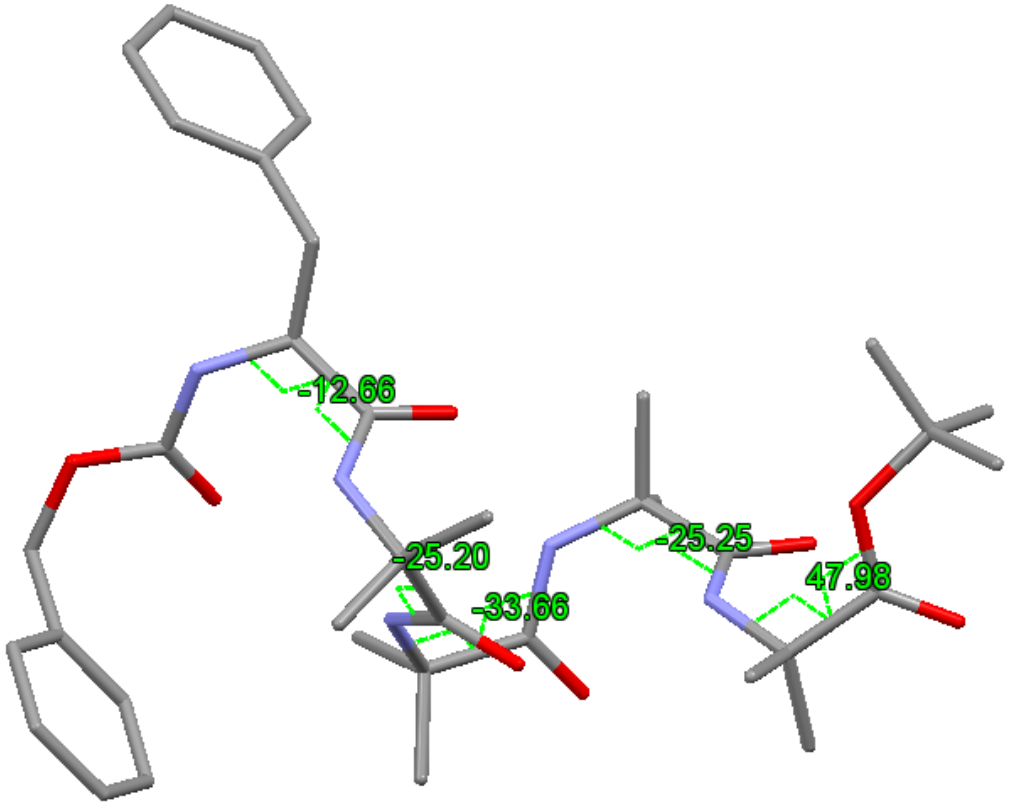

Figure S28. Highlighting the ϕ torsion angles for one molecule in the unit cell for Cbz-Phe-$(Aib)_4$-O^{t}Bu.

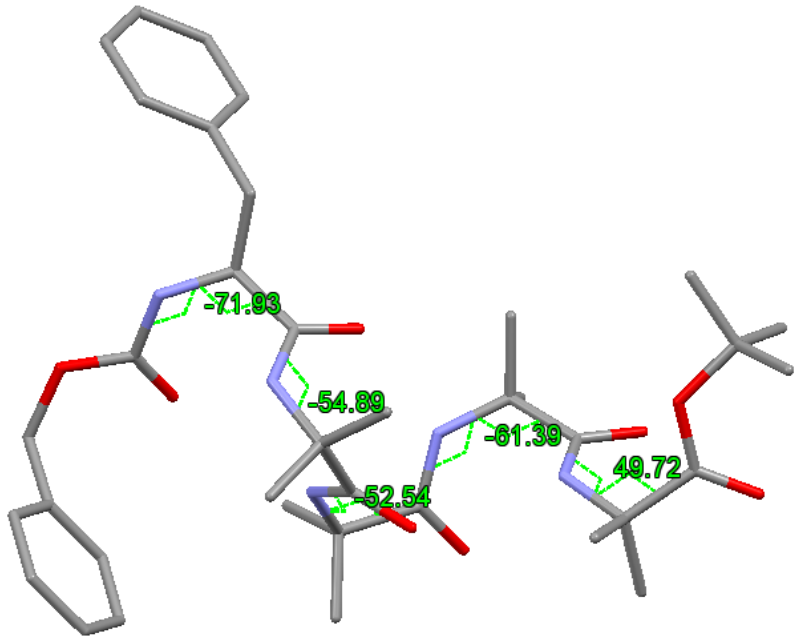

Figure S29. Highlighting the ψ torsion angles for one molecule in the unit cell for Cbz-Phe-$(Aib)_4$-O^{t}Bu.

Intramolecular Hydrogen-bonding interactions in Cbz-Phe-$(Aib)_4$-O^{t}Bu

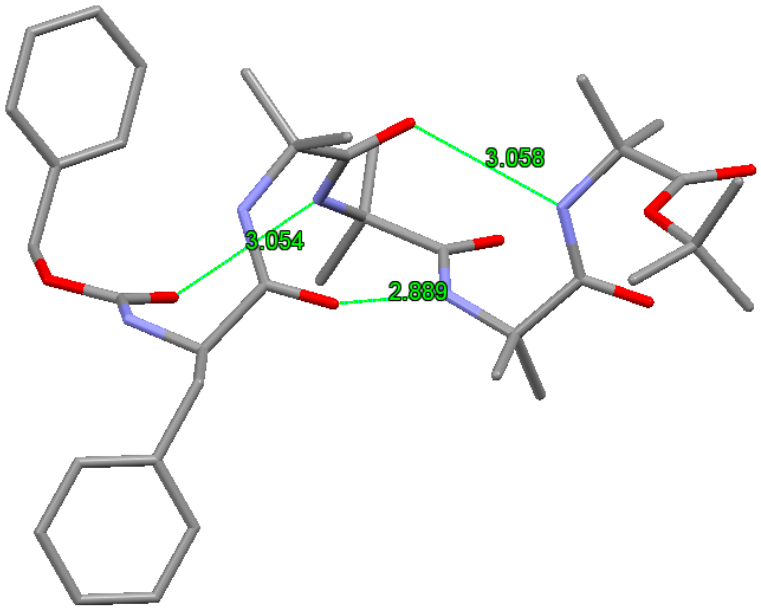

Figure S30. Intramolecular hydrogen bonding interactions present in Cbz-Phe-$(Aib)_4$-O^{t}Bu.

Intermolecular π-π stacking interactions in Cbz-L-Phe-$(Aib)_4$-O^{t}Bu.

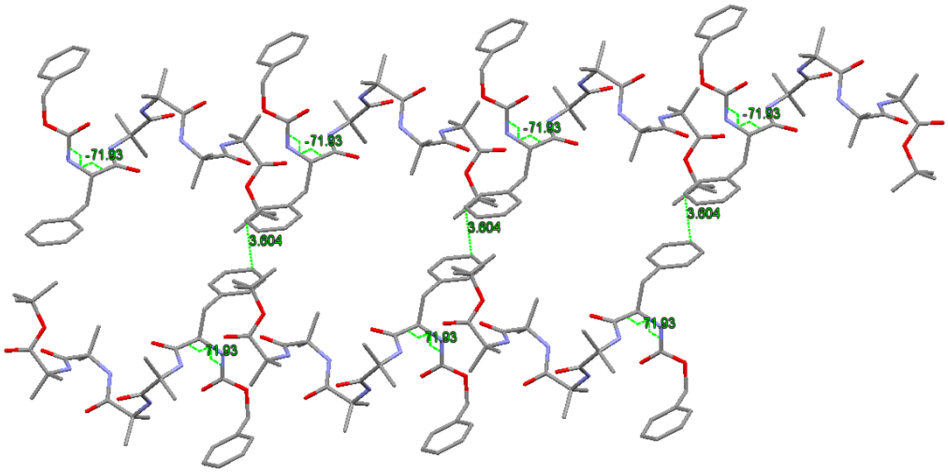

Figure S31. Intermolecular π-π stacking interactions present in Cbz-Phe-$(Aib)_4$-O^{t}Bu between peptides of opposite screw-sense.

Packing of *M* and *P* Helices in Cbz-L-Phe-$(Aib)_4$-O^{t}Bu.

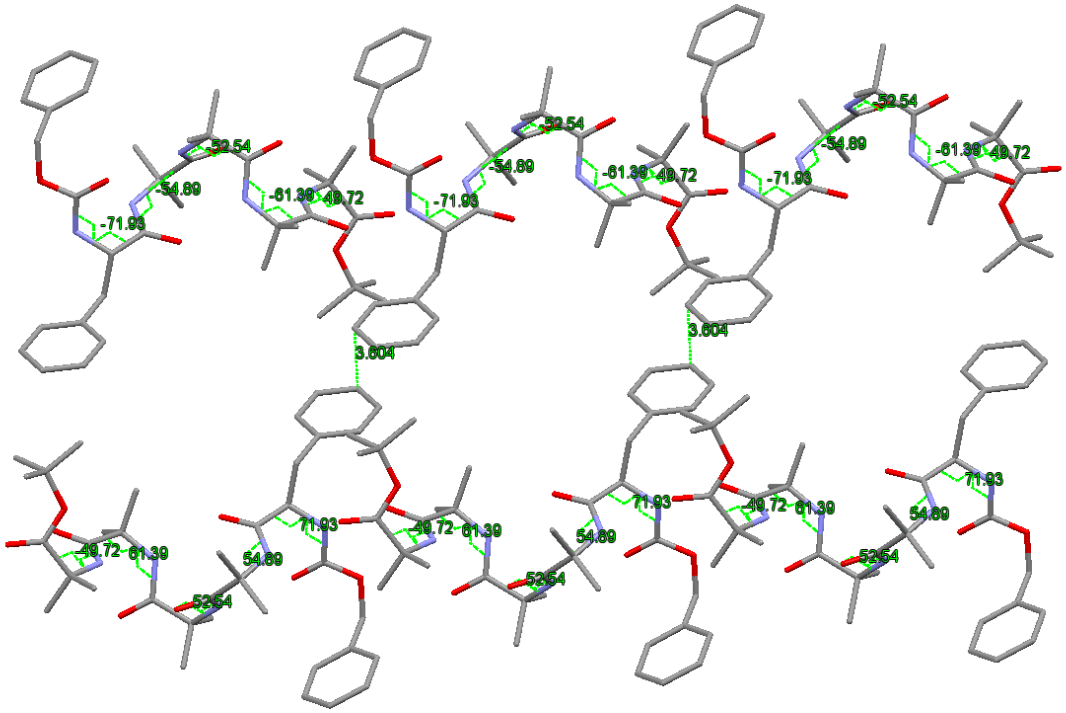

Figure S32. Arrangement of *M* and *P* helices in the solid-state for Cbz-Phe-$(Aib)_4$-O^{t}Bu.

Crystal Structure Data for N_3-$(Aib)_4$-$GlyNH_2$

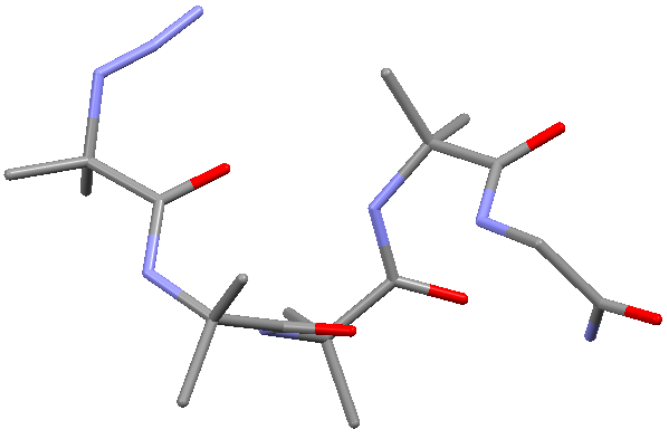

Table S6. Crystal data and structure refinement for N_3-$(Aib)_4$-$GlyNH_2$

Identification code	N_3-$(Aib)_4$-$GlyNH_2$
Empirical formula	C19 H36 N8 O6
Formula weight	472.56

Temperature	100(2) K
Wavelength	1.5418 A
Crystal system, space group	Triclinic, P-1
Unit cell dimensions	a = 8.5578(6) alpha = 71.838(7) b = 10.4202(9) beta = 82.558(6) c = 15.1810(11) gamma = 74.669(7)
Volume	1238.90(17) A^3
Z, Calculated density	2, 1.267 Mg/m^3
Absorption coefficient	0.797 mm^-1
F(000)	508
Crystal size	0.21 x 0.19 x 0.17 mm
Theta range for data collection	3.0651 to 74.0840 deg.
Limiting indices	-10<=h<=9, -12<=k<=12, -18<=l<=16
Reflections collected / unique	9925 / 4630 [R(int) = 0.0290]
Completeness to theta = 66.60	96.5 %
Absorption correction	Semi-empirical from equivalents
Max. and min. transmission	1.00000 and 0.58868
Refinement method	Full-matrix least-squares on F^2
Data / restraints / parameters	4630 / 0 / 333
Goodness-of-fit on F^2	1.056
Final R indices [I>2sigma(I)]	R1 = 0.0435, wR2 = 0.1191
R indices (all data)	R1 = 0.0481, wR2 = 0.1240
Extinction coefficient	0.0041(6)
Largest diff. peak and hole	0.867 and -0.411 e.A^-3

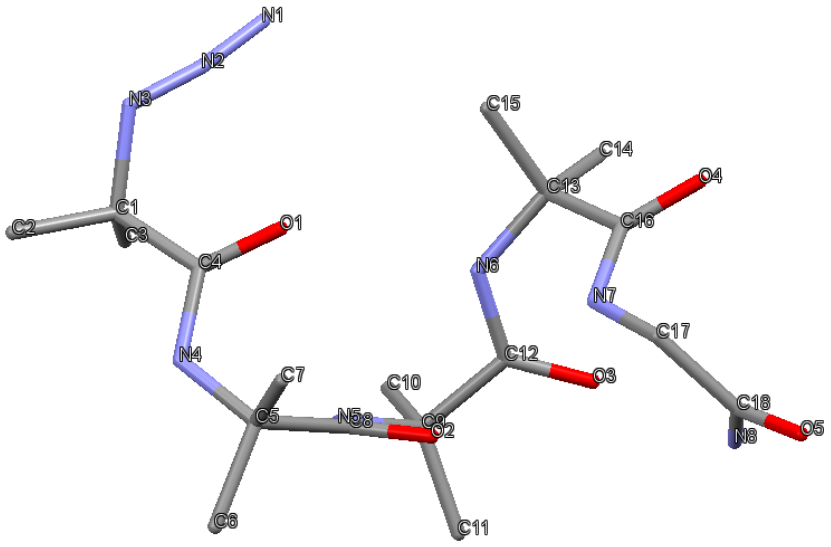

Table S7. Torsion angles [deg] for N_3-(Aib)$_4$-GlyNH_2

N(3)-C(1)-C(4)-O(1)	-31.43(18)
C(2)-C(1)-C(4)-O(1)	-146.59(14)
C(3)-C(1)-C(4)-O(1)	89.15(16)
N(3)-C(1)-C(4)-N(4)	153.10(13)
C(2)-C(1)-C(4)-N(4)	37.95(19)
C(3)-C(1)-C(4)-N(4)	-86.32(16)
N(4)-C(5)-C(8)-O(2)	149.33(13)
C(7)-C(5)-C(8)-O(2)	26.84(18)
C(6)-C(5)-C(8)-O(2)	-92.87(16)
N(4)-C(5)-C(8)-N(5)	-31.59(17)
C(7)-C(5)-C(8)-N(5)	-154.08(13)
C(6)-C(5)-C(8)-N(5)	86.20(15)
N(5)-C(9)-C(12)-O(3)	144.74(14)
C(11)-C(9)-C(12)-O(3)	21.6(2)
C(10)-C(9)-C(12)-O(3)	-98.14(16)
N(5)-C(9)-C(12)-N(6)	-40.08(18)
C(11)-C(9)-C(12)-N(6)	-163.22(14)
C(10)-C(9)-C(12)-N(6)	77.05(16)
N(6)-C(13)-C(16)-O(4)	160.53(13)
C(14)-C(13)-C(16)-O(4)	37.43(19)
C(15)-C(13)-C(16)-O(4)	-82.38(17)
N(6)-C(13)-C(16)-N(7)	-24.04(18)
C(14)-C(13)-C(16)-N(7)	-147.14(13)
C(15)-C(13)-C(16)-N(7)	93.05(15)
N(7)-C(17)-C(18)-O(5)	172.41(14)
N(7)-C(17)-C(18)-N(8)	-7.9(2)
N(1)-N(2)-N(3)-C(1)	166.9(11)
C(2)-C(1)-N(3)-N(2)	-168.97(14)
C(3)-C(1)-N(3)-N(2)	-48.85(19)
C(4)-C(1)-N(3)-N(2)	68.94(17)
O(1)-C(4)-N(4)-C(5)	0.7(2)
C(1)-C(4)-N(4)-C(5)	176.02(12)
C(7)-C(5)-N(4)-C(4)	68.69(17)
C(6)-C(5)-N(4)-C(4)	-170.95(13)
C(8)-C(5)-N(4)-C(4)	-53.27(18)
O(2)-C(8)-N(5)-C(9)	-0.2(2)

C(5)-C(8)-N(5)-C(9)	-179.21(12)
C(11)-C(9)-N(5)-C(8)	76.84(17)
C(10)-C(9)-N(5)-C(8)	-162.57(13)
C(12)-C(9)-N(5)-C(8)	-46.40(18)
O(3)-C(12)-N(6)-C(13)	2.2(2)
C(9)-C(12)-N(6)-C(13)	-172.90(13)
C(14)-C(13)-N(6)-C(12)	65.35(18)
C(15)-C(13)-N(6)-C(12)	-174.49(14)
C(16)-C(13)-N(6)-C(12)	-58.30(18)
O(4)-C(16)-N(7)-C(17)	-2.4(2)
C(13)-C(16)-N(7)-C(17)	-177.70(12)
C(18)-C(17)-N(7)-C(16)	-83.05(18)

Table S8. Hydrogen bonds for N_3-$(Aib)_4$-$GlyNH_2$ [A and deg.].

D-H...A	d(D-H)	d(H...A)	d(D...A)	<(DHA)
N(8)-H(8B)...O(3)#1	0.90(2)	2.06(2)	2.9604(17)	174(2)
N(8)-H(8A)...O(3)	0.89(2)	2.17(2)	3.0498(19)	171(2)
N(5)-H(5)...O(6)#2	0.84(2)	2.11(2)	2.9249(18)	163(2)
N(4)-H(4)...O(4)#3	0.91(2)	2.15(2)	3.0342(17)	165.2(18)
N(7)-H(7)...O(2)	0.82(2)	2.09(2)	2.8880(18)	162(2)
N(6)-H(6)...O(1)	0.83(2)	2.20(2)	2.9957(17)	162(2)
O(6)-H(6D)...O(5)#1	0.84	1.87	2.6956(17)	167.9

Torsion angles for N_3-$(Aib)_4$-$GlyNH_2$

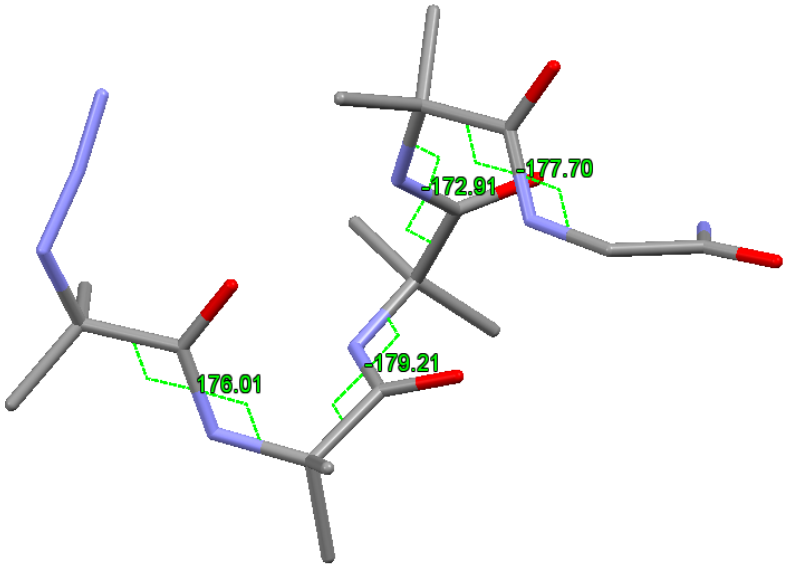

Figure S33. Highlighting the ω torsion angles for one molecule in the unit cell for N_3-$(Aib)_4$-$GlyNH_2$.

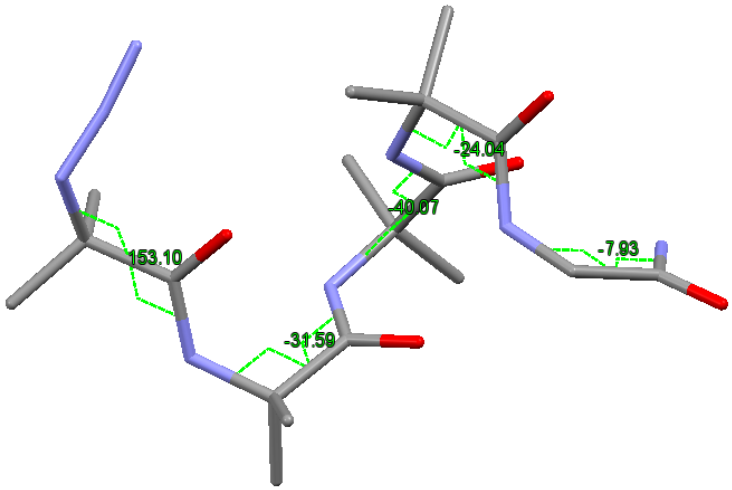

Figure S34. Highlighting the ϕ torsion angles for one molecule in the unit cell for N_3-$(Aib)_4$-$GlyNH_2$.

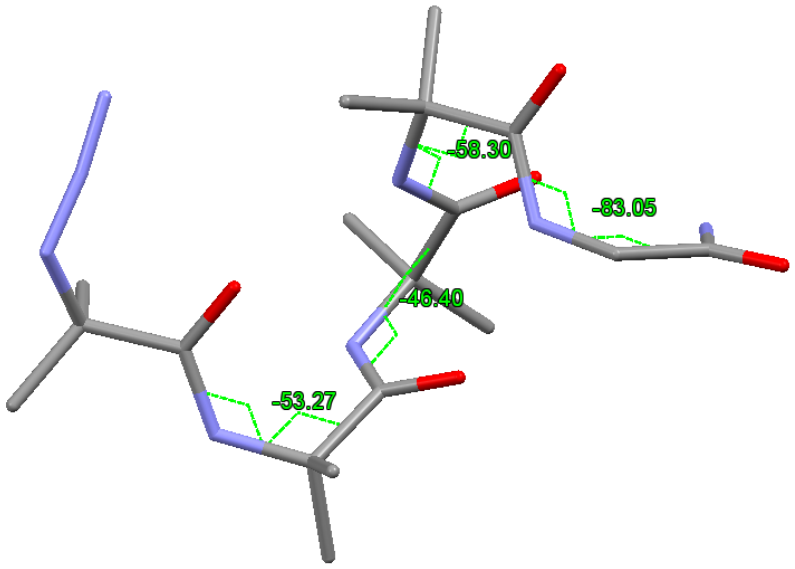

Figure S35. Highlighting the ψ torsion angles for one molecule in the unit cell for N_3-$(Aib)_4$-$GlyNH_2$.

Intramolecular Hydrogen-bonding interactions in N_3-$(Aib)_4$-$GlyNH_2$

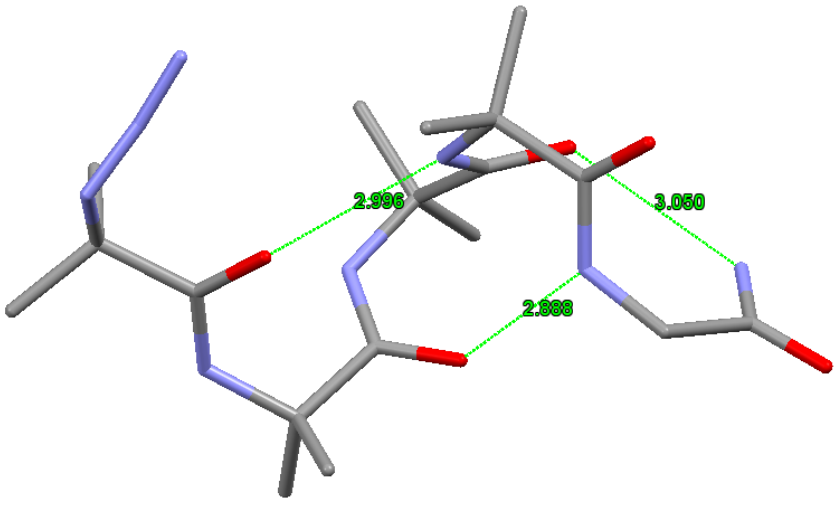

Figure S36. Intramolecular hydrogen bonding interactions present in one molecule of N_3-$(Aib)_4$-$GlyNH_2$ found in the unit cell.

Packing of *M* and *P* Helices in N_3-$(Aib)_4$-$GlyNH_2$

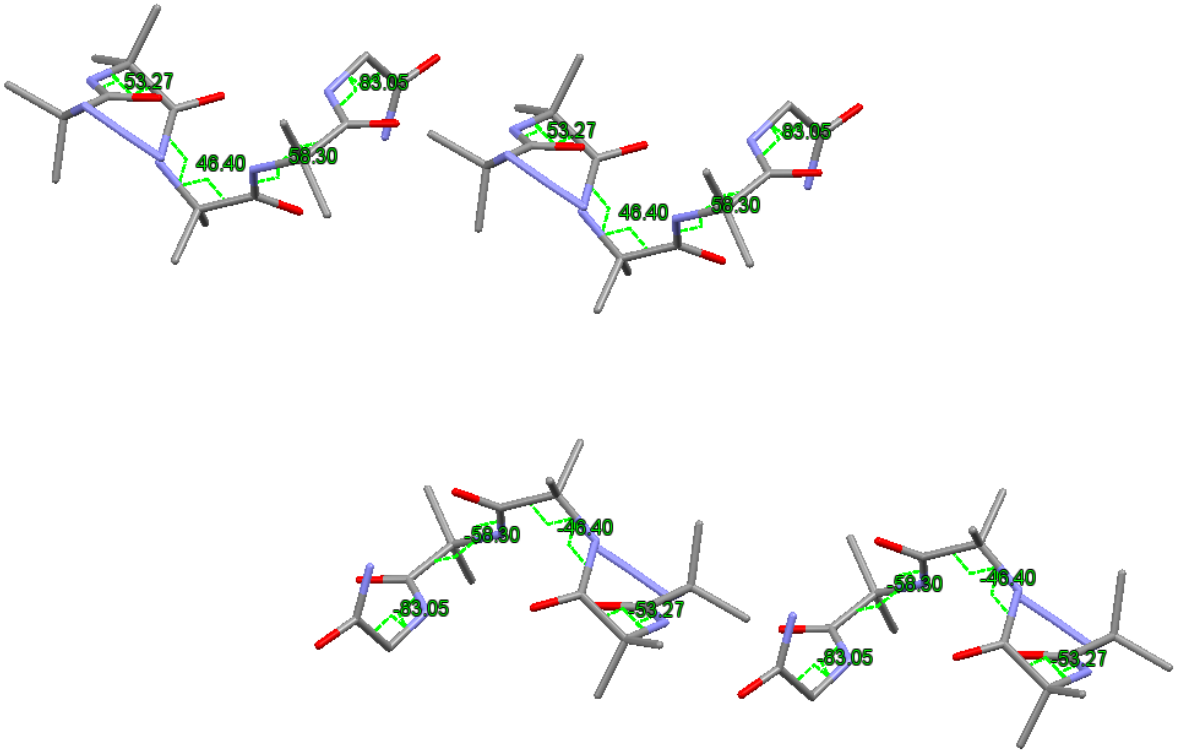

Figure S37. Arrangement of *M* and *P* helices in the solid-state for N_3-$(Aib)_4$-$GlyNH_2$.

Crystal data for Cbz-L-Phe-$(Aib)_4$-Ac_5c-$(Aib)_4$-$GlyNH_2$

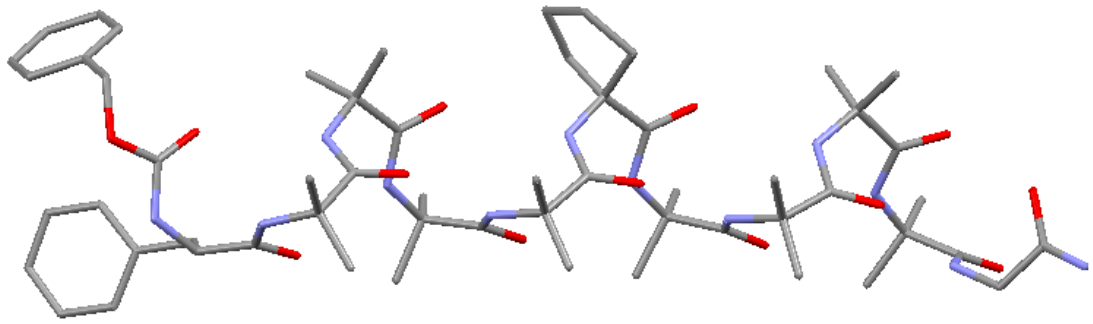

Table S9. Crystal data and structure refinement for Cbz-L-Phe-$(Aib)_4$-Ac_5c-$(Aib)_4$-$GlyNH_2$

Identification code	Cbz-L-Phe-$(Aib)_4$-Ac_5c-$(Aib)_4$-$GlyNH_2$
Empirical formula	C57 H88.50 N12 O14.25
Formula weight	1169.90
Temperature	100(2) K

Wavelength	0.71073 A
Crystal system, space group	Monoclinic, $P2_1$
Unit cell dimensions	a = 13.774(7) alpha = 90 b = 9.540(5) beta = 94.375(9) c = 48.58(2) gamma = 90
Volume	6365(6) A^3
Z, Calculated density	4, 1.221 Mg/m^3
Absorption coefficient	0.089 mm^-1
F(000)	2514
Crystal size	0.65 x 0.45 x 0.15 mm
Theta range for data collection	1.76 to 23.26 deg.
Limiting indices	-15<=h<=15, -10<=k<=10, -52<=l<=53
Reflections collected / unique	39207 / 18208 [R(int) = 0.1564]
Completeness to theta = 23.26	99.9 %
Absorption correction	None
Refinement method	Full-matrix least-squares on F^2
Data / restraints / parameters	18208 / 2000 / 1639
Goodness-of-fit on F^2	1.083
Final R indices [I>2sigma(I)]	R1 = 0.1288, wR2 = 0.3080
R indices (all data)	R1 = 0.1610, wR2 = 0.3294
Largest diff. peak and hole	0.809 and -0.466 e.A^-3

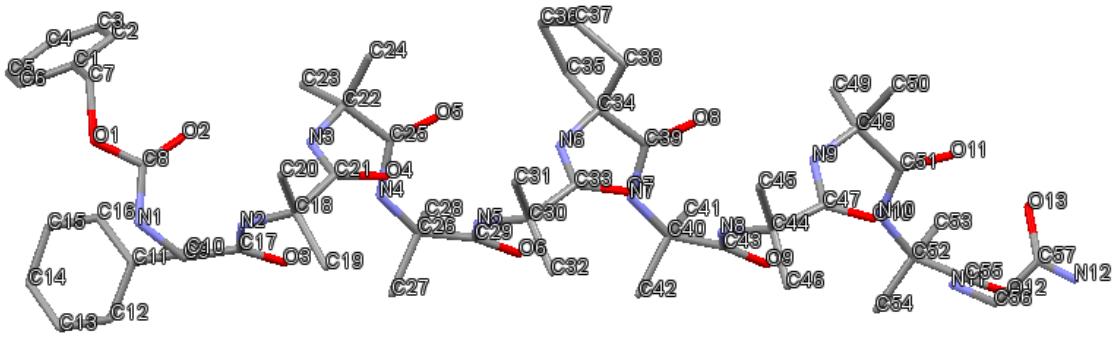

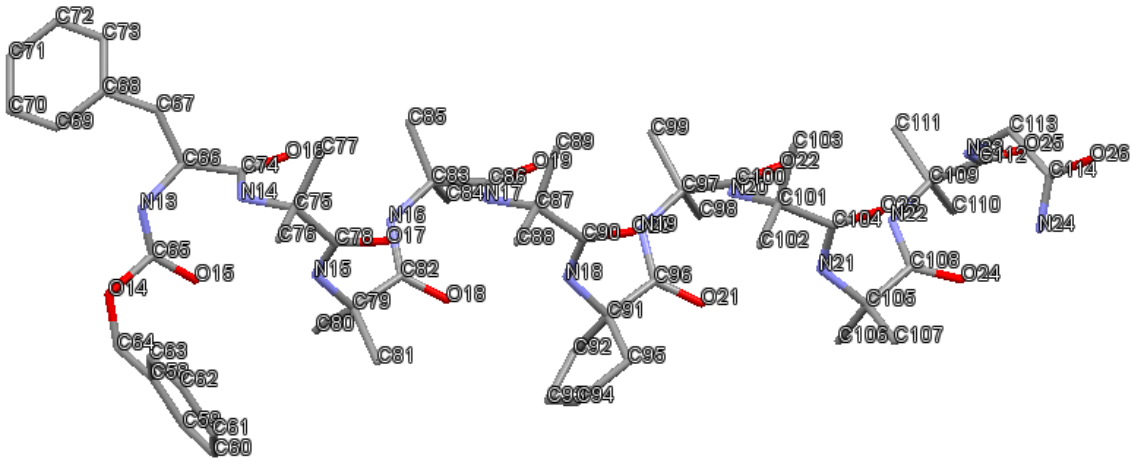

Table S10. Hydrogen bonds for Cbz-L-Phe-(Aib)$_4$-Ac$_5$c-(Aib)$_4$-GlyNH$_2$ [A and deg.].

D-H...A	d(D-H)	d(H...A)	d(D...A)	<(DHA)
N(1)-H(1N)...O(26)#1	0.88	1.98	2.849(8)	168.6
N(2)-H(2N)...O(1S)#2	0.88	2.14	3.009(10)	167.7
N(3)-H(3N)...O(2)	0.88	2.18	3.050(10)	170.1
N(4)-H(4N)...O(3)	0.88	2.11	2.974(9)	165.1
N(5)-H(5N)...O(4)	0.88	2.10	2.941(13)	159.0
N(6)-H(6N)...O(5)	0.88	2.13	3.007(10)	171.3
N(7)-H(7N)...O(6)	0.88	2.14	3.012(10)	168.6
N(8)-H(8N)...O(7)	0.88	1.99	2.840(13)	161.8
N(9)-H(9N)...O(8)	0.88	2.13	3.007(12)	172.3
N(10)-H(10N)...O(9)	0.88	2.12	2.956(12)	158.8
N(11)-H(11N)...O(10)	0.88	2.15	2.876(11)	139.5
N(12)-H(12A)...O(2S)	0.88	2.06	2.74(3)	133.8
N(13)-H(13N)...O(2S)#3	0.88	2.77	3.19(3)	110.8
N(14)-H(14N)...O(2S)#3	0.88	2.15	2.97(3)	154.8
N(15)-H(15N)...O(15)	0.88	2.20	3.044(17)	160.3
N(16)-H(16N)...O(16)	0.88	2.16	3.021(15)	164.9
N(17)-H(17N)...O(17)	0.88	2.08	2.927(14)	162.4
N(18)-H(18N)...O(18)	0.88	2.09	2.958(12)	170.5
N(19)-H(19N)...O(19)	0.88	2.13	2.987(11)	165.1
N(20)-H(20N)...O(20)	0.88	2.09	2.895(12)	151.1
N(21)-H(21N)...O(21)	0.88	2.13	3.002(10)	174.0
N(22)-H(22N)...O(22)	0.88	2.11	2.947(9)	159.2
N(23)-H(23N)...O(23)	0.88	2.08	2.884(10)	151.3
N(24)-H(24E)...O(24)	0.88	2.12	2.963(9)	159.9

Torsion angles for Cbz-L-Phe-(Aib)$_4$-Ac$_5$c-(Aib)$_4$-GlyNH$_2$

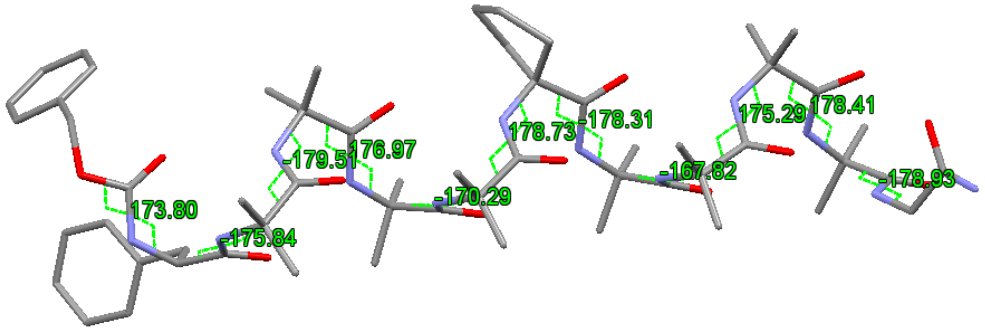

Figure S38. Highlighting the ω torsion angles for one molecule in the unit cell for Cbz-L-Phe-(Aib)$_4$-Ac$_5$c-(Aib)$_4$-GlyNH$_2$.

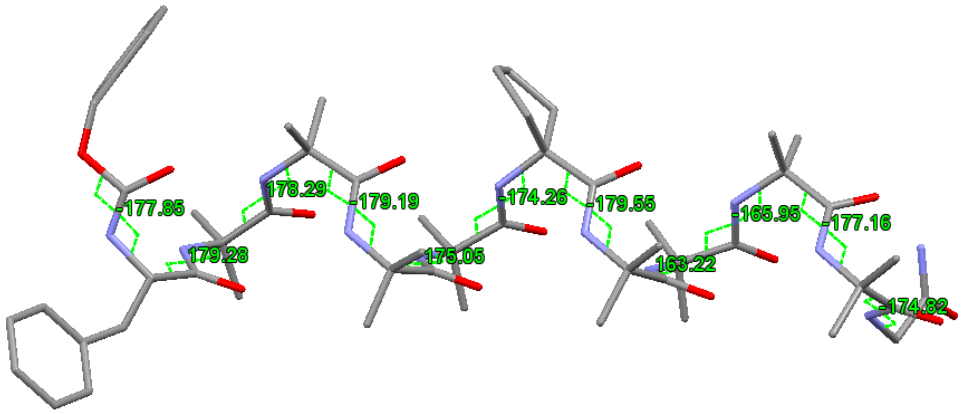

Figure S39. Highlighting the ω torsion angles for one molecule in the unit cell for Cbz-L-Phe-(Aib)$_4$-Ac$_5$c-(Aib)$_4$-GlyNH$_2$.

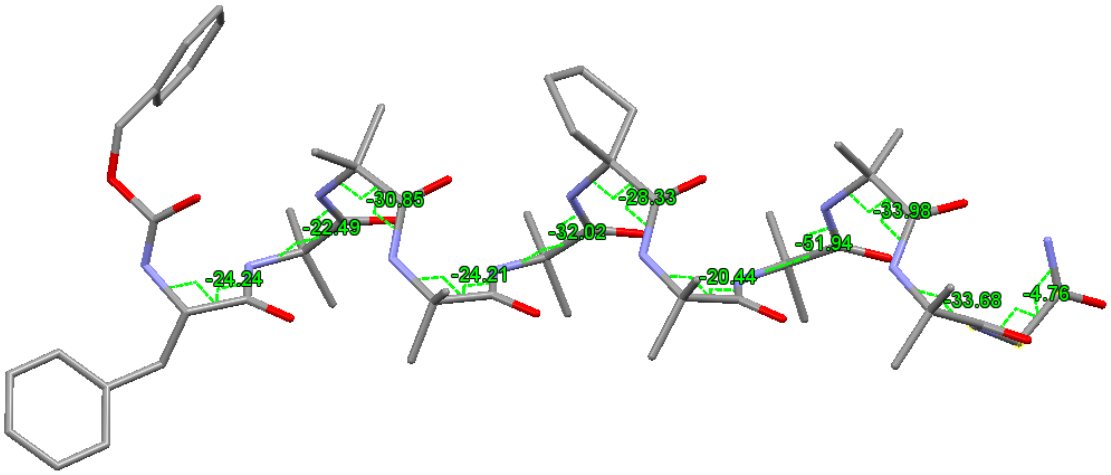

Figure S40. Highlighting the ϕ torsion angles for one molecule in the unit cell for Cbz-L-Phe-(Aib)$_4$-Ac$_5$c-(Aib)$_4$-GlyNH$_2$.

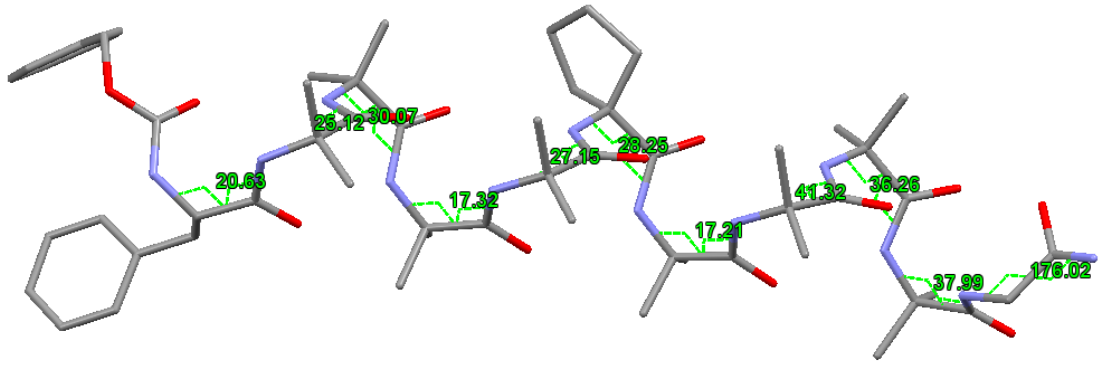

Figure S41. Highlighting the ϕ torsion angles for one molecule in the unit cell for Cbz-L-Phe-$(Aib)_4$-Ac_5c-$(Aib)_4$-$GlyNH_2$.

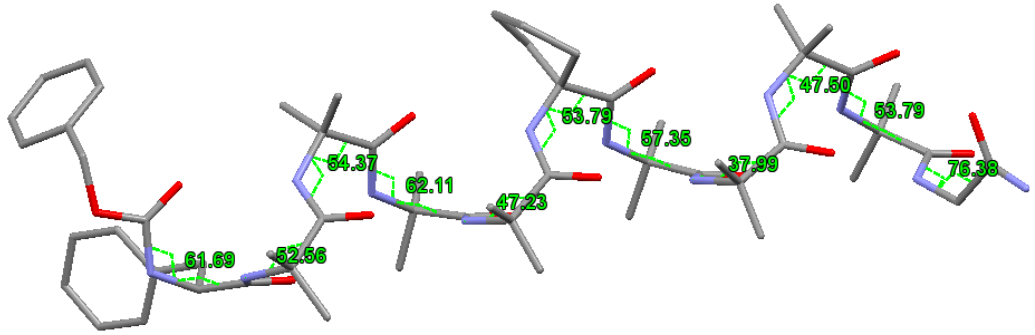

Figure S42. Highlighting the ψ torsion angles for one molecule in the unit cell for Cbz-L-Phe-$(Aib)_4$-Ac_5c-$(Aib)_4$-$GlyNH_2$.

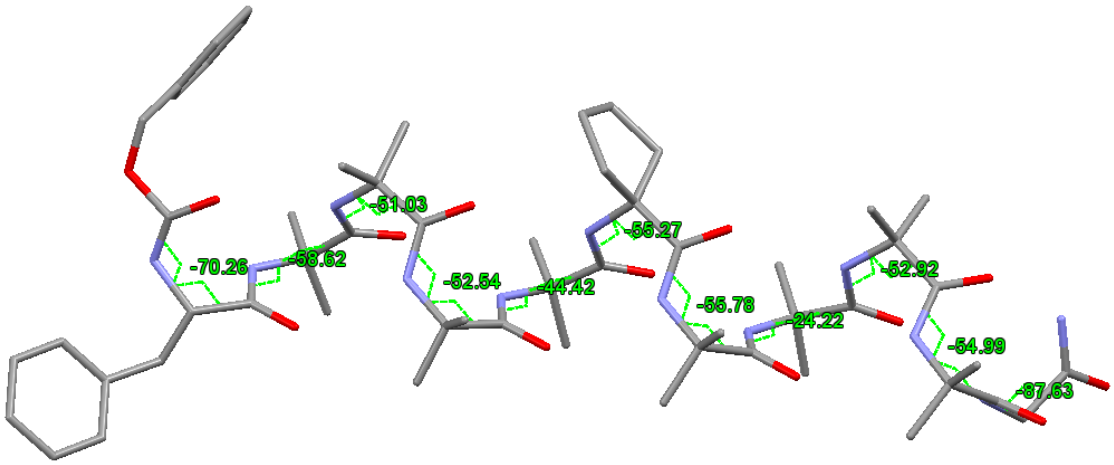

Figure S43. Highlighting the ψ torsion angles for one molecule in the unit cell for Cbz-L-Phe-$(Aib)_4$-Ac_5c-$(Aib)_4$-$GlyNH_2$.

Intramolecular Hydrogen-bonding interactions in Cbz-L-Phe-$(Aib)_4$-Ac_5c-$(Aib)_4$-$GlyNH_2$.

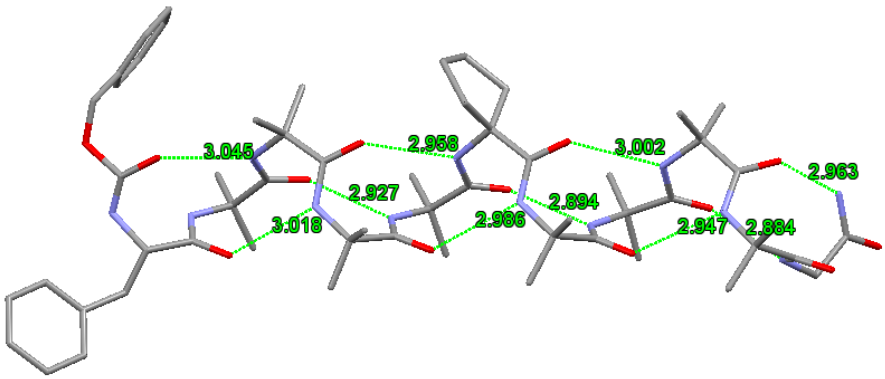

Figure S44. Intramolecular hydrogen bonding interactions present in one molecule of Cbz-L-Phe-$(Aib)_4$-Ac_5c-$(Aib)_4$-$GlyNH_2$ in the unit cell.

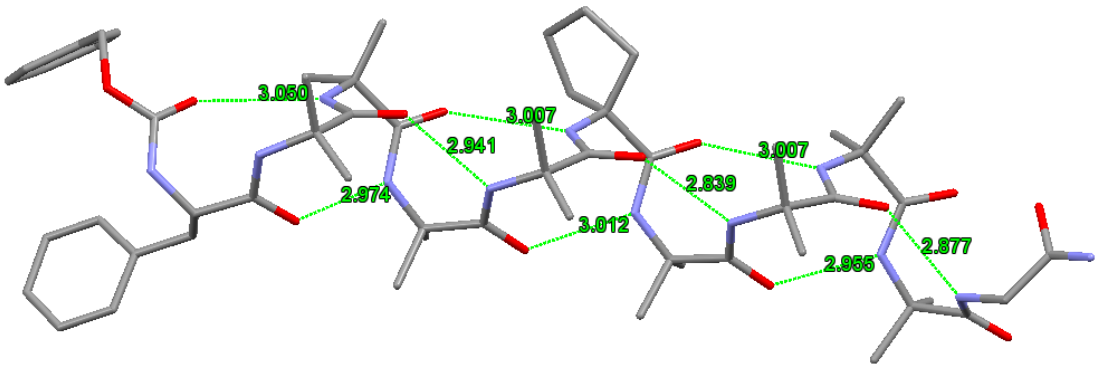

Figure S45. Intramolecular hydrogen bonding interactions present in one molecule of Cbz-L-Phe-$(Aib)_4$-Ac_5c-$(Aib)_4$-$GlyNH_2$ found in the unit cell.

Packing of Cbz-L-Phe-$(Aib)_4$-Ac_5c-$(Aib)_4$-$GlyNH_2$ in the unit cell

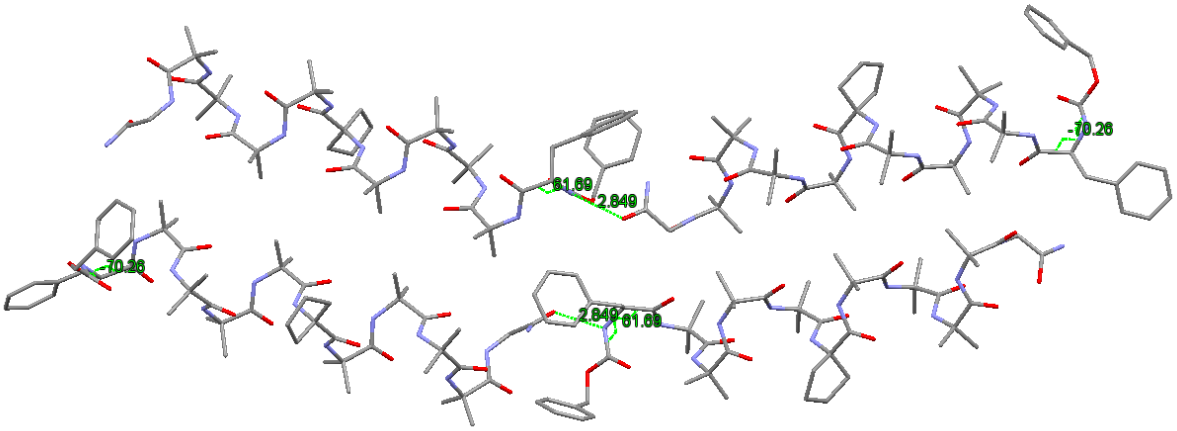

Figure S46. Intermolecular hydrogen bonding interactions present between two molecules of Cbz-L-Phe-$(Aib)_4$-Ac_5c-$(Aib)_4$-$GlyNH_2$ of the opposite screw-sense preference found in the unit cell.

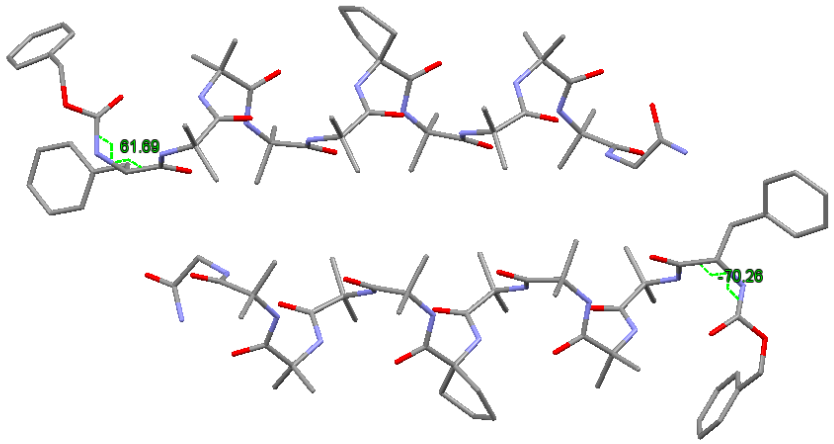

Figure S47. Packing of Cbz-L-Phe-$(Aib)_4$-Ac_5c-$(Aib)_4$-$GlyNH_2$ in the unit cell displaying pseudo-symmetry with a non-crystallographic C_2 axis.

Length of 3_{10} Helical Conformation in Cbz-L-Phe-$(Aib)_4$-Ac_5c-$(Aib)_4$-$GlyNH_2$

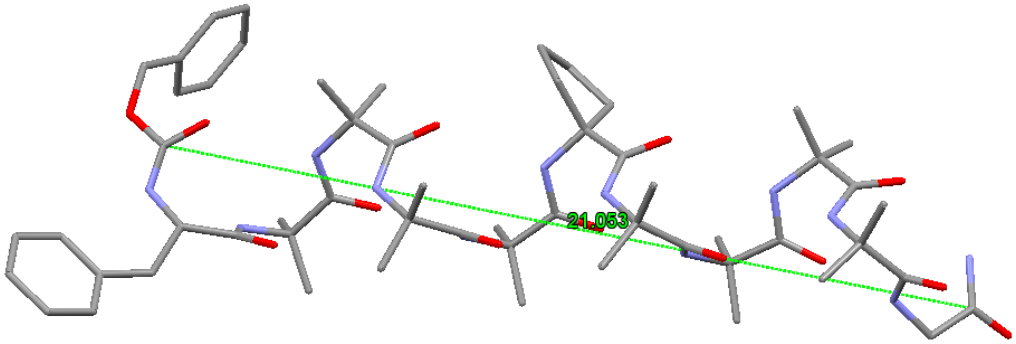

Figure S48. Length of 3_{10} helical conformation adopted by Cbz-L-Phe-$(Aib)_4$-Ac_5c-$(Aib)_4$-$GlyNH_2$ for one molecule in the unit cell.

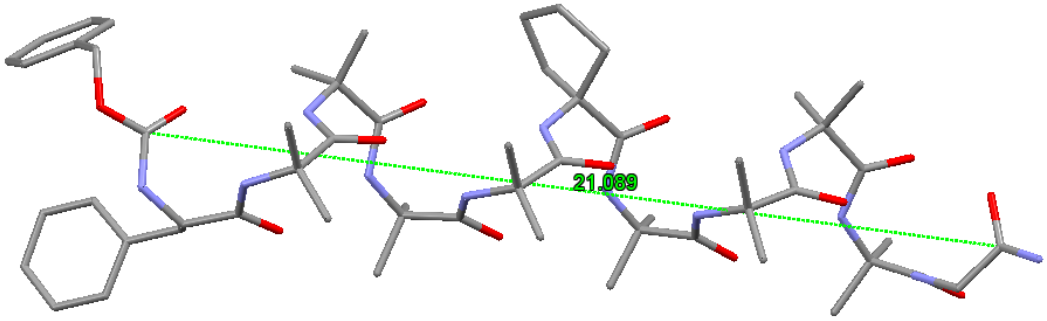

Figure S49. Length of 3_{10} helical conformation adopted by Cbz-L-Phe-$(Aib)_4$-Ac_5c-$(Aib)_4$-$GlyNH_2$ for one molecule in the unit cell.

Crystal data for Cbz-L-Phe-$(Aib)_4$-Ac_6c-$(Aib)_4$-$GlyNH_2$.

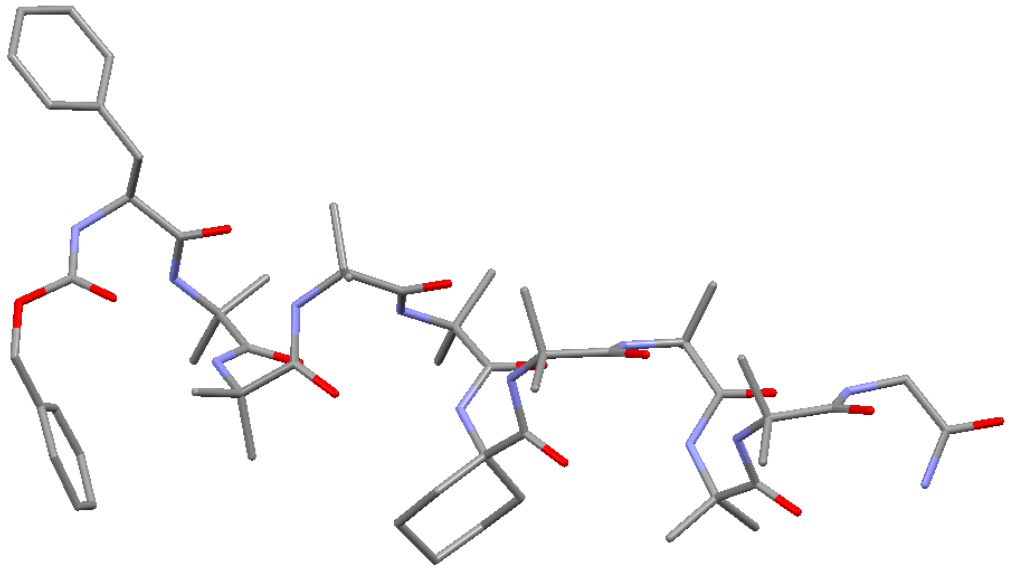

Table S11. Crystal data and structure refinement for Cbz-L-Phe-$(Aib)_4$-Ac_6c-$(Aib)_4$-$GlyNH_2$.

Identification code	Cbz-L-Phe-$(Aib)_4$-Ac_6c-$(Aib)_4$-$GlyNH_2$.
Empirical formula	C232 H356 N48 O54
Formula weight	4681.65
Temperature	100(2) K
Wavelength	0.71073 A
Crystal system, space group	Monoclinic, $P2_{(1)}$
Unit cell dimensions	a = 18.316(6) alpha = 90 b = 17.553(6) beta = 96.012(6) c = 20.359(7) gamma = 90
Volume	6509(4) A^3
Z, Calculated density	1, 1.194 Mg/m^3
Absorption coefficient	0.086 mm^-1
F(000)	2516
Crystal size	0.50 x 0.40 x 0.15 mm
Theta range for data collection	2.20 to 25.03 deg.
Limiting indices	-21<=h<=21, -20<=k<=20, -24<=l<=24
Reflections collected / unique	45952 / 11842 [R(int) = 0.1228]

Completeness to theta = 25.03	99.6 %
Absorption correction	None
Refinement method	Full-matrix least-squares on F^2
Data / restraints / parameters	11842 / 8 / 1539
Goodness-of-fit on F^2	1.115
Final R indices [I>2sigma(I)]	R1 = 0.0852, wR2 = 0.1972
R indices (all data)	R1 = 0.1472, wR2 = 0.2173
Largest diff. peak and hole	0.490 and -0.319 e.A^-3

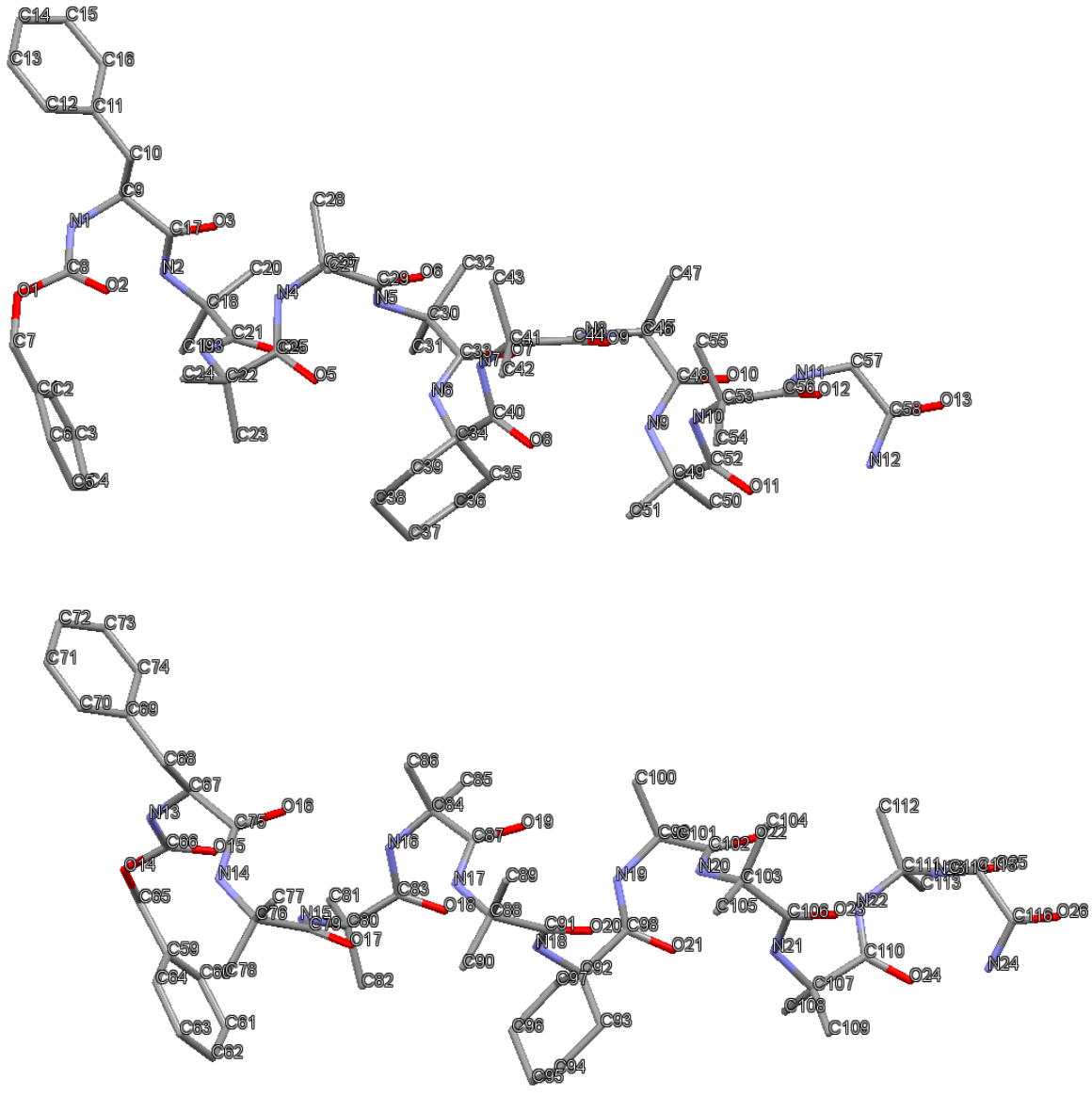

Table S12. Hydrogen bonds for Cbz-L-Phe-$(Aib)_4$-Ac_6c-$(Aib)_4$-$GlyNH_2$. [A and deg.].

D-H...A	d(D-H)	d(H...A)	d(D...A)	<(DHA)
N(12)-H(12N)...O(11)	0.88(2)	2.14(3)	3.012(12)	171(12)
N(23)-H(23N)...O(23)	0.88	2.04	2.865(12)	155.0
N(22)-H(22N)...O(22)	0.88	2.17	3.023(12)	161.9
N(21)-H(21N)...O(21)	0.88	2.13	2.958(13)	157.2
N(20)-H(20N)...O(20)	0.88	2.31	3.156(11)	160.2
N(19)-H(19N)...O(19)	0.88	2.16	2.993(12)	157.1
N(18)-H(18N)...O(18)	0.88	2.18	3.005(12)	154.8
N(17)-H(17N)...O(17)	0.88	2.14	2.980(11)	160.6
N(16)-H(16N)...O(16)	0.88	2.15	2.995(12)	161.5
N(15)-H(15N)...O(15)	0.88	2.23	3.038(11)	152.7
N(14)-H(14N)...O(13)#1	0.88	2.08	2.881(12)	150.2
N(13)-H(13N)...O(12)#1	0.88	1.98	2.829(11)	160.4
N(11)-H(11N)...O(10)	0.88	2.07	2.926(11)	163.5
N(10)-H(10N)...O(9)	0.88	2.07	2.912(11)	160.0
N(9)-H(9N)...O(8)	0.88	2.06	2.910(11)	161.3
N(8)-H(8N)...O(7)	0.88	2.28	3.108(11)	157.3
N(7)-H(7N)...O(6)	0.88	2.16	2.963(12)	150.8
N(6)-H(6N)...O(5)	0.88	2.26	3.056(11)	150.3
N(5)-H(5N)...O(4)	0.88	2.15	2.953(11)	151.2
N(4)-H(4N)...O(3)	0.88	2.19	3.004(11)	154.3
N(3)-H(3N)...O(2)	0.88	2.21	2.970(10)	144.6
N(2)-H(2N)...O(26)#2	0.88	2.11	2.958(11)	162.9
N(1)-H(1N)...O(25)#2	0.88	2.04	2.899(11)	166.3

Torsion angles for Cbz-L-Phe-(Aib)$_4$-Ac$_6$c-(Aib)$_4$-GlyNH$_2$.

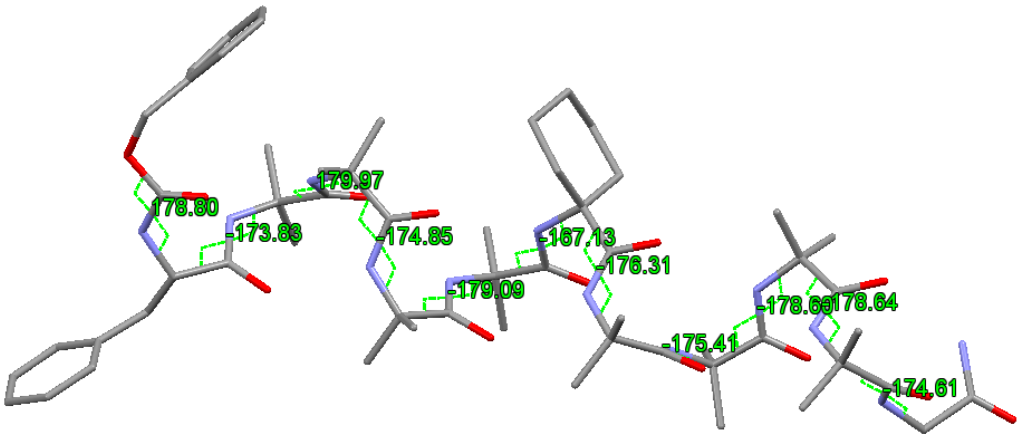

Figure S50. Highlighting the ω torsion angles for one molecule in the unit cell for Cbz-L-Phe-(Aib)$_4$-Ac$_6$c-(Aib)$_4$-GlyNH$_2$.

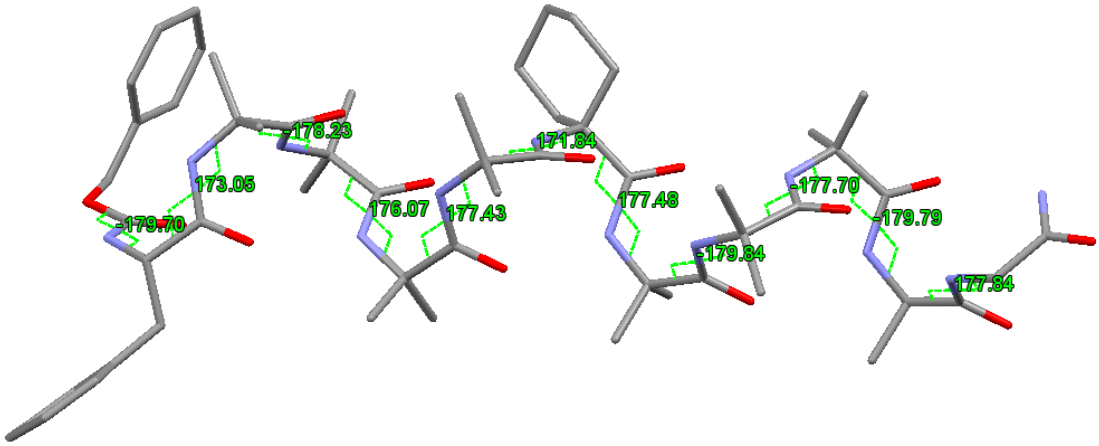

Figure S51. Highlighting the ω torsion angles for one molecule in the unit cell for Cbz-L-Phe-(Aib)$_4$-Ac$_6$c-(Aib)$_4$-GlyNH$_2$.

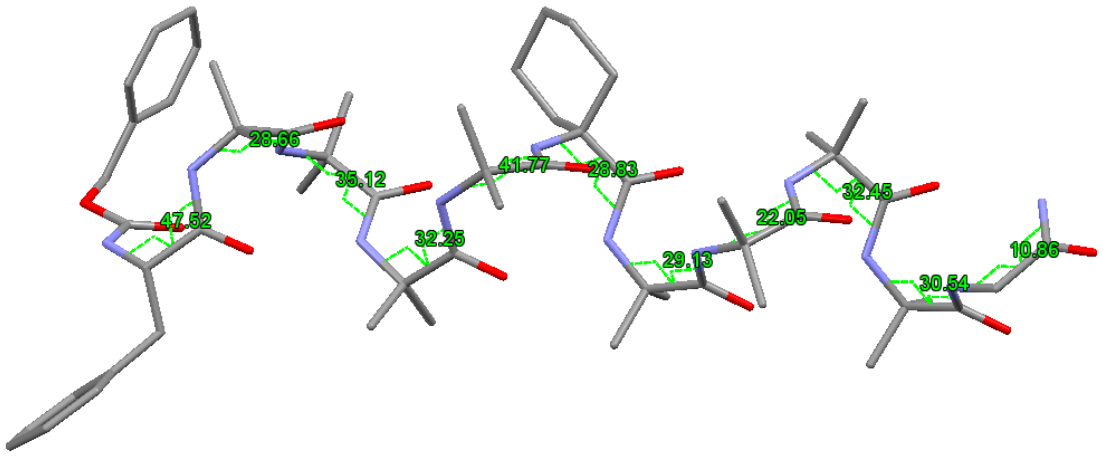

Figure S52. Highlighting the ϕ torsion angles for one molecule in the unit cell for Cbz-L-Phe-$(Aib)_4$-Ac_6c-$(Aib)_4$-$GlyNH_2$.

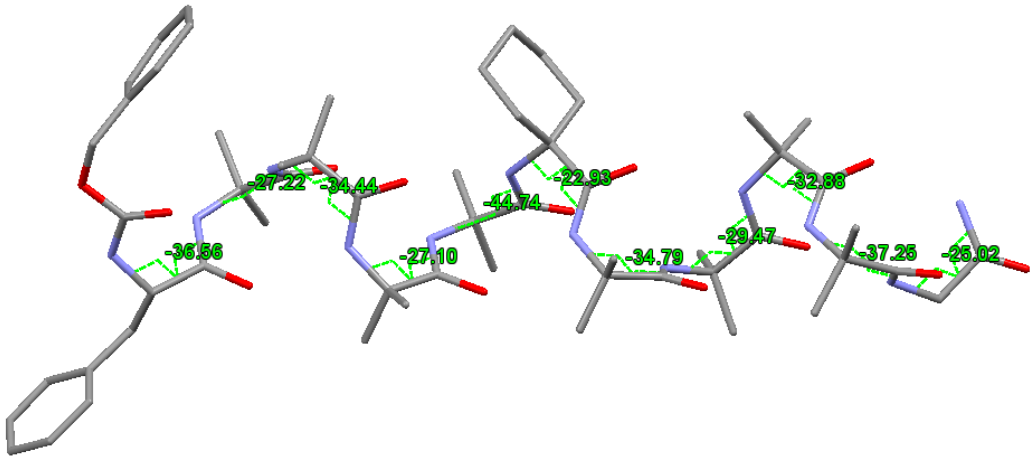

Figure S53. Highlighting the ϕ torsion angles for one molecule in the unit cell for Cbz-L-Phe-$(Aib)_4$-Ac_6c-$(Aib)_4$-$GlyNH_2$.

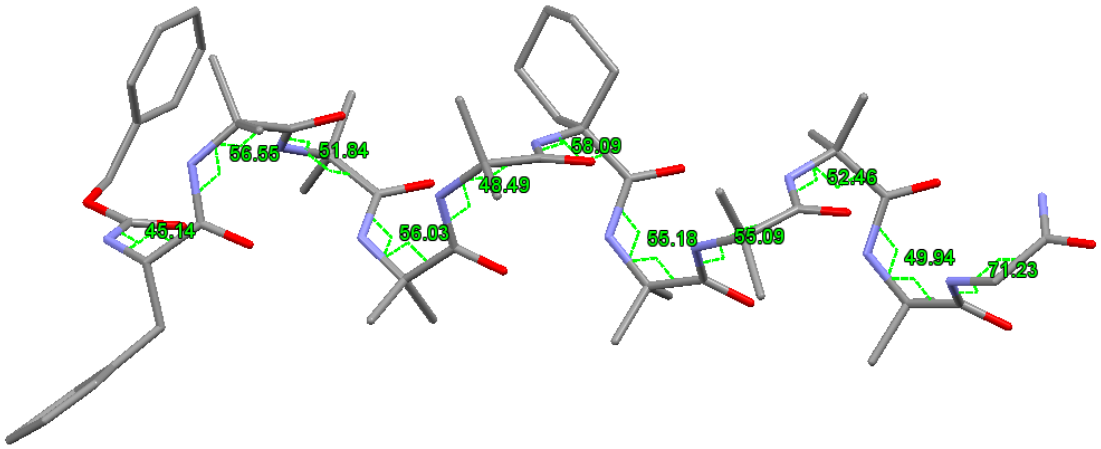

Figure S54. Highlighting the Ψ torsion angles for one molecule in the unit cell for Cbz-L-Phe-$(Aib)_4$-Ac_6c-$(Aib)_4$-$GlyNH_2$.

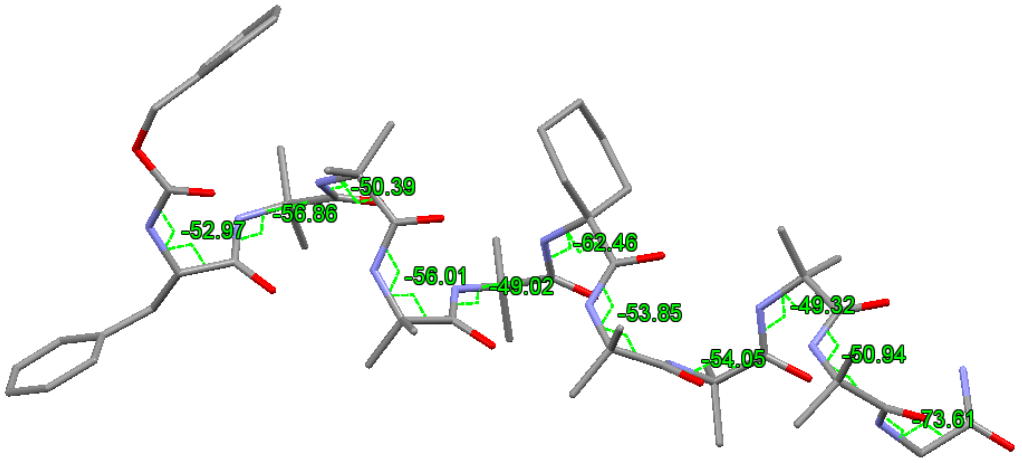

Figure S55. Highlighting the Ψ torsion angles for one molecule in the unit cell for Cbz-L-Phe-$(Aib)_4$-Ac_6c-$(Aib)_4$-$GlyNH_2$.

Intramolecular Hydrogen-bonding interactions in Cbz-L-Phe-$(Aib)_4$-Ac_6c-$(Aib)_4$-$GlyNH_2$.

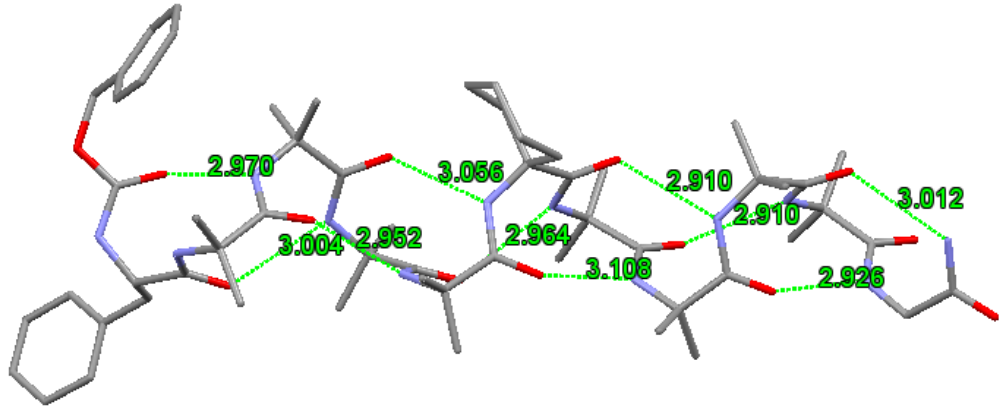

Figure S56. Intramolecular hydrogen bonding interactions present in one molecule of Cbz-L-Phe-$(Aib)_4$-Ac_6c-$(Aib)_4$-$GlyNH_2$. found in the unit cell.

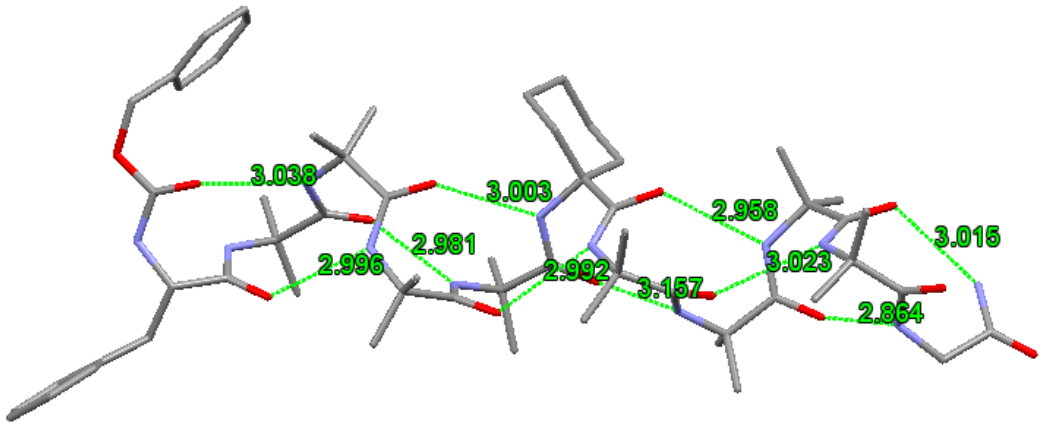

Figure S57. Intramolecular hydrogen bonding interactions present in one molecule of Cbz-L-Phe-$(Aib)_4$-Ac_6c-$(Aib)_4$-$GlyNH_2$. found in the unit cell.

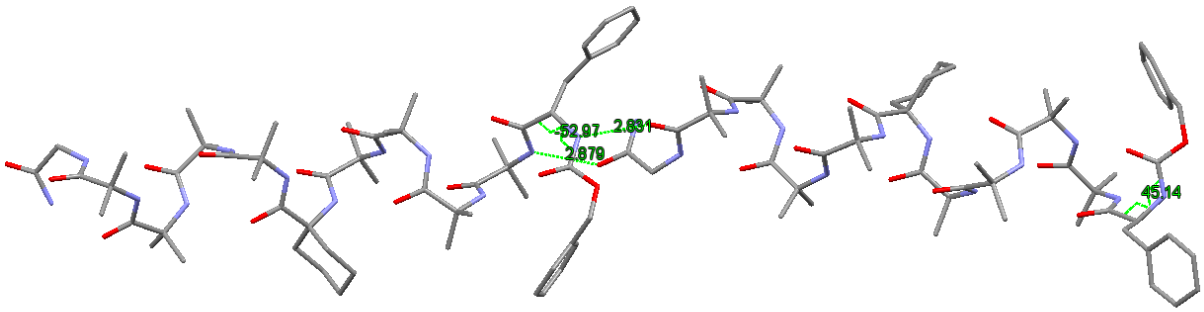

Figure S58. Intermolecular hydrogen bonding interactions present between two molecules of Cbz-L-Phe-$(Aib)_4$-Ac_6c-$(Aib)_4$-$GlyNH_2$ of the opposite screw-sense preference found in the unit cell.

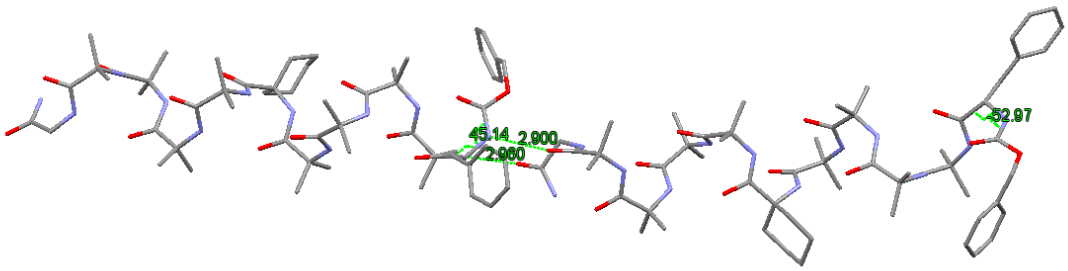

Figure S59. Intermolecular hydrogen bonding interactions present between two molecules of Cbz-L-Phe-$(Aib)_4$-Ac_6c-$(Aib)_4$-$GlyNH_2$ of the opposite screw-sense preference found in the unit cell.

Packing of Cbz-L-Phe-$(Aib)_4$-Ac_6c-$(Aib)_4$-$GlyNH_2$ in the unit cell

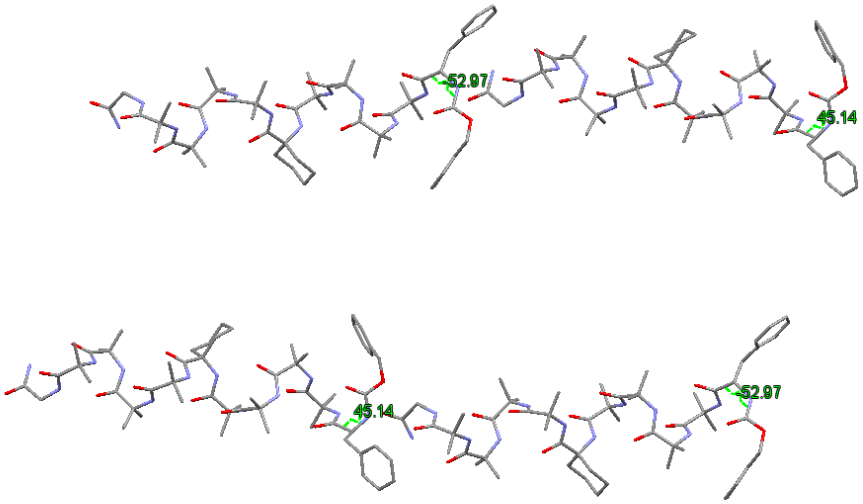

Figure S60. Packing of Cbz-L-Phe-$(Aib)_4$-Ac_6c-$(Aib)_4$-$GlyNH_2$ in the unit cell displaying no pseudo-symmetric C_2 axis.

Length of 3_{10} Helical Conformation in Cbz-L-Phe-$(Aib)_4$-Ac_6c-$(Aib)_4$-$GlyNH_2$.

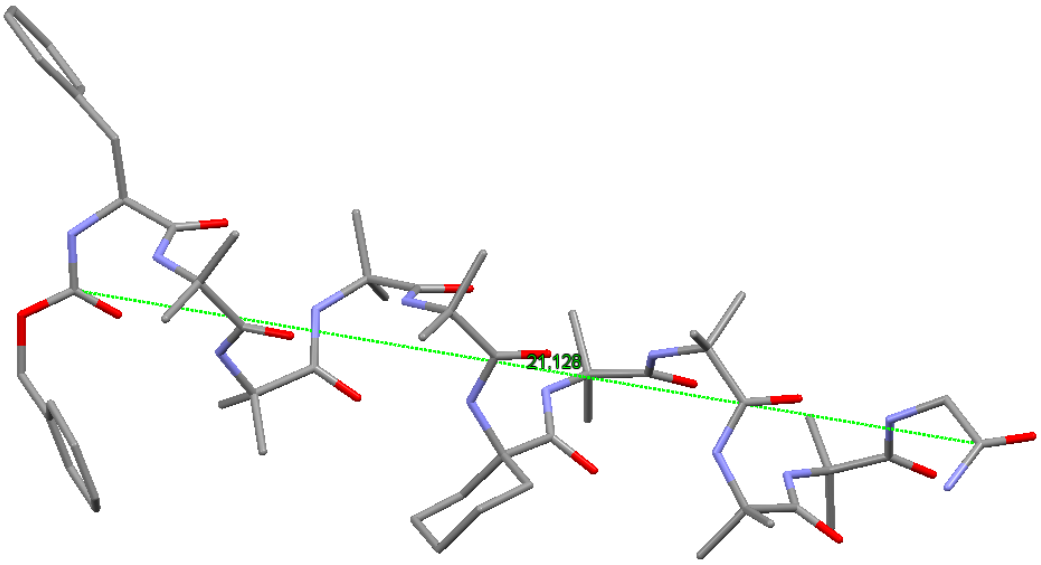

Figure S61. Length of 3_{10} helical conformation adopted by Cbz-L-Phe-$(Aib)_4$-Ac_6c-$(Aib)_4$-$GlyNH_2$ for one molecule in the unit cell.

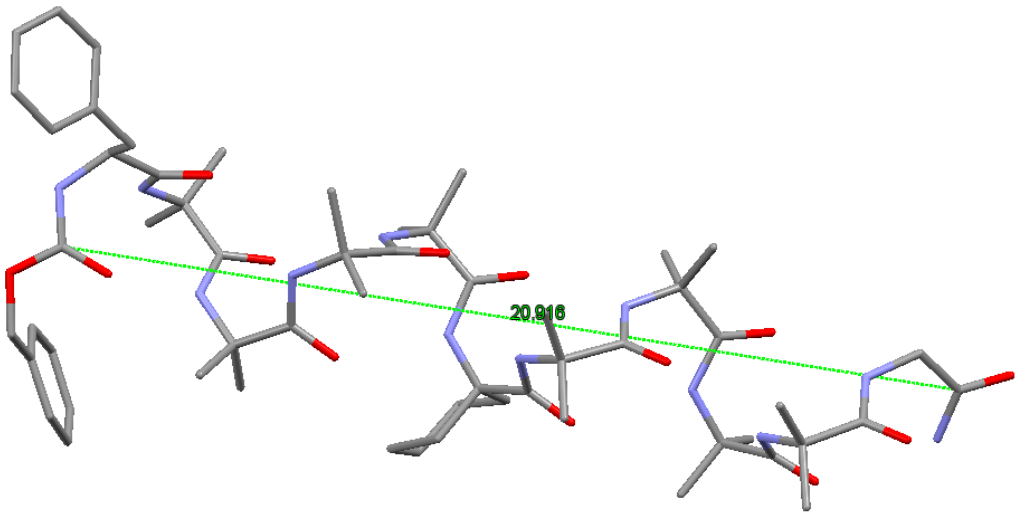

Figure S62. Length of 3_{10} helical conformation adopted by Cbz-L-Phe-$(Aib)_4$-Ac_6c-$(Aib)_4$-$GlyNH_2$ for one molecule in the unit cell.

Table S13. Crystal data and structure refinement for Cbz-L-Phe-$(Aib)_4$-Bip-$(Aib)_4$-$GlyNH_2$.

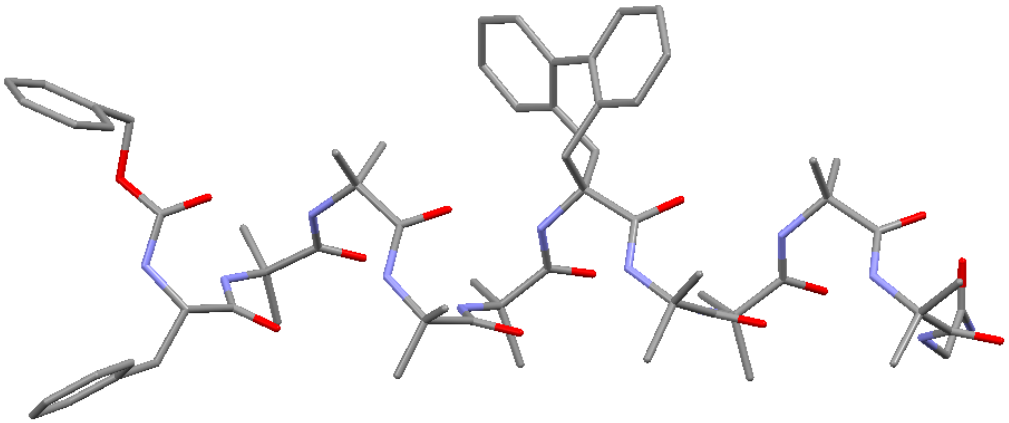

Identification code	Cbz-L-Phe-$(Aib)_4$-Bip-$(Aib)_4$-$GlyNH_2$
Empirical formula	C67.50 H97 N12 O16
Formula weight	1332.57
Temperature	100(2) K
Wavelength	0.71073 A
Crystal system, space group	Monoclinic, P2(1)
Unit cell dimensions	a = 19.474(6) alpha = 90 b = 13.389(4) beta = 95.638(5) c = 28.731(9) gamma = 90
Volume	7455(4) A^3
Z, Calculated density	4, 1.187 Mg/m^3
Absorption coefficient	0.085 mm^-1
F(000)	2856
Crystal size	0.60 x 0.25 x 0.08 mm
Theta range for data collection	2.08 to 20.82 deg.
Limiting indices	-19<=h<=19, -13<=k<=13, -28<=l<=28
Reflections collected / unique	35778 / 8239 [R(int) = 0.1609]
Completeness to theta = 20.82	99.9 %
Absorption correction	None
Refinement method	Full-matrix least-squares on F^2
Data / restraints / parameters	8239 / 2941 / 1663
Goodness-of-fit on F^2	1.095
Final R indices [I>2sigma(I)]	R1 = 0.1202, wR2 = 0.2993

R indices (all data)	R1 = 0.1818, wR2 = 0.3417
Largest diff. peak and hole	0.586 and -0.450 e.A^-3

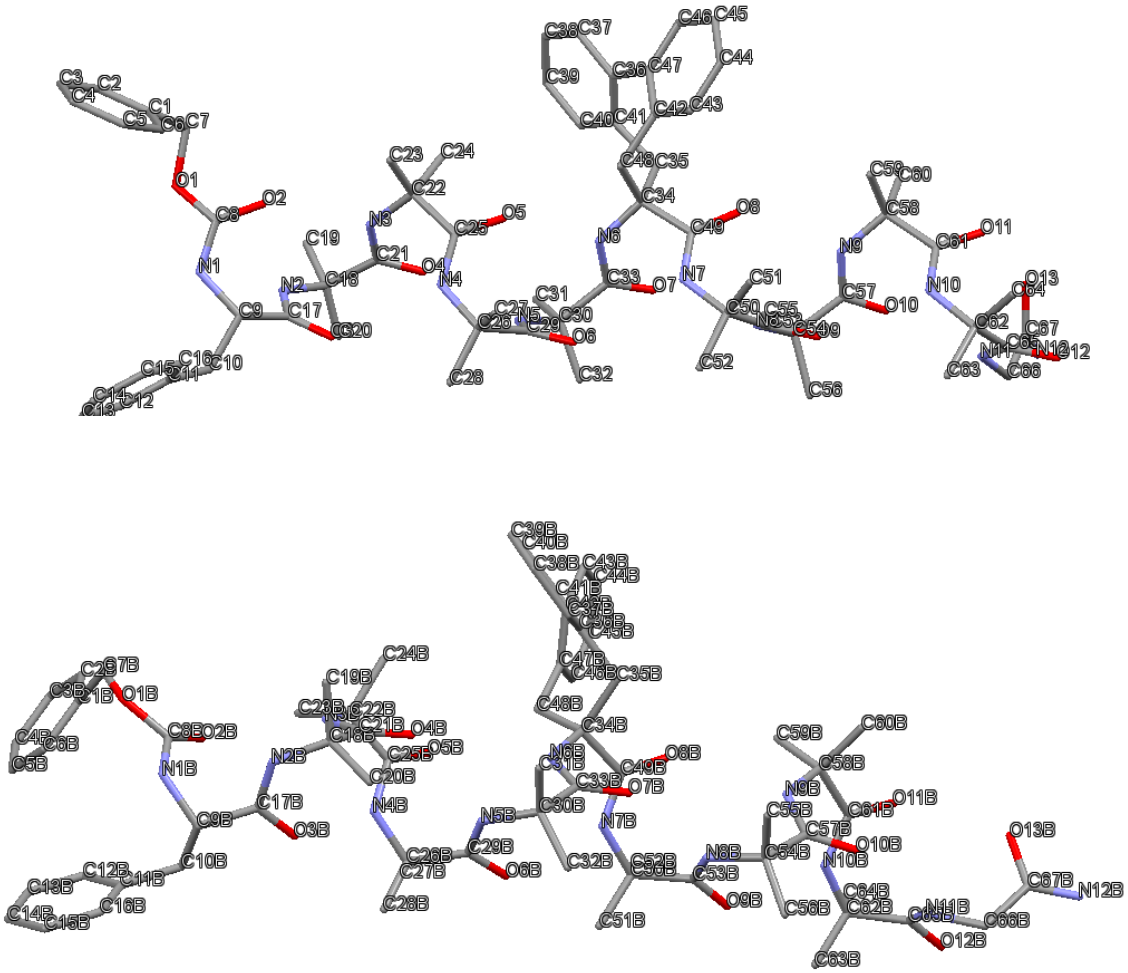

Table S14. Hydrogen bonds for Cbz-L-Phe-$(Aib)_4$-Bip-$(Aib)_4$-$GlyNH_2$ [A and deg.].

D-H...A	d(D-H)	d(H...A)	d(D...A)	<(DHA)
N(12B)-H(12F)...N(12)#1	0.88	2.97	3.66(3)	136.2
N(12B)-H(12F)...O(13)#1	0.88	2.55	3.10(2)	121.7
N(12B)-H(12E)...O(1S)#2	0.88	2.03	2.84(2)	152.1
N(11B)-H(11B)...O(10B)	0.88	2.21	3.07(2)	165.2
N(10B)-H(10M)...O(9B)	0.88	2.11	2.968(17)	164.3
N(9B)-H(9BN)...O(8B)	0.88	2.13	2.990(15)	164.6
N(8B)-H(8BN)...O(7B)	0.88	2.16	3.019(16)	166.5
N(7B)-H(7BN)...O(6B)	0.88	2.22	3.073(15)	161.9
N(6B)-H(6BN)...O(5B)	0.88	2.11	2.954(15)	160.6
N(5B)-H(5BN)...O(4B)	0.88	2.10	2.910(17)	152.8
N(4B)-H(4BN)...O(3B)	0.88	2.16	2.994(18)	159.1
N(3B)-H(3BN)...O(2B)	0.88	2.17	2.97(2)	150.1

N(1B)-H(1BN)...O(12B)#3	0.88	2.04	2.83(2)	149.0
N(12)-H(12A)...N(12B)#4	0.88	3.01	3.66(3)	132.2
N(11)-H(11N)...O(10)	0.88	1.94	2.733(19)	149.0
N(10)-H(10N)...O(9)	0.88	2.16	3.002(17)	159.8
N(9)-H(9N)...O(8)	0.88	2.11	2.983(15)	171.8
N(8)-H(8N)...O(7)	0.88	2.07	2.922(16)	162.2
N(7)-H(7N)...O(6)	0.88	2.25	3.097(15)	162.0
N(6)-H(6N)...O(5)	0.88	2.06	2.917(15)	164.2
N(4)-H(4N)...O(3)	0.88	2.20	3.053(16)	163.0
N(3)-H(3N)...O(2)	0.88	2.18	3.040(18)	166.1
N(1)-H(1N)...O(12)#5	0.88	2.12	2.947(19)	155.8
N(5)-H(5N)...O(4)	0.88	2.04	2.870(16)	157.3

Torsion angles for Cbz-L-Phe-$(Aib)_4$-Bip-$(Aib)_4$-$GlyNH_2$

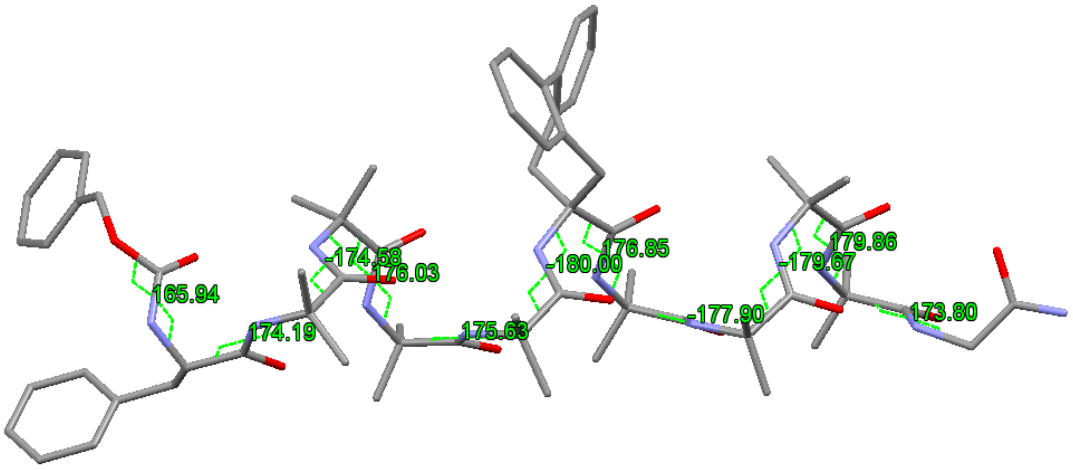

Figure S63. Highlighting the ω torsion angles for one molecule in the unit cell for Cbz-L-Phe-$(Aib)_4$-Bip-$(Aib)_4$-$GlyNH_2$.

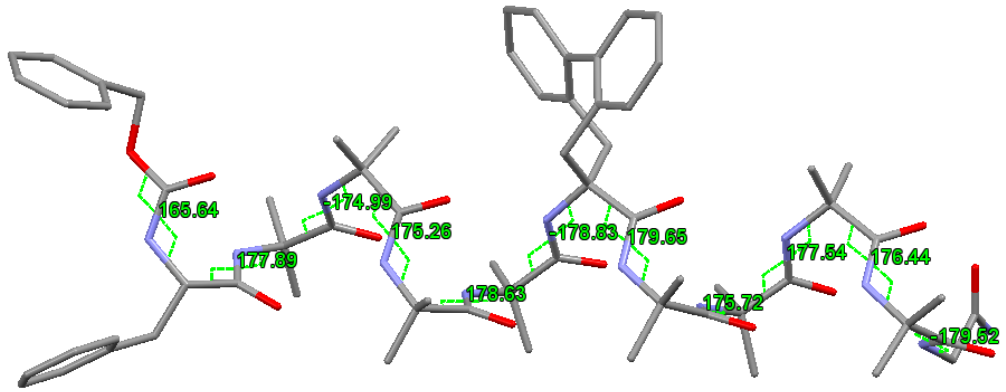

Figure S64. Highlighting the ω torsion angles for one molecule in the unit cell for Cbz-L-Phe-$(Aib)_4$-Bip-$(Aib)_4$-$GlyNH_2$.

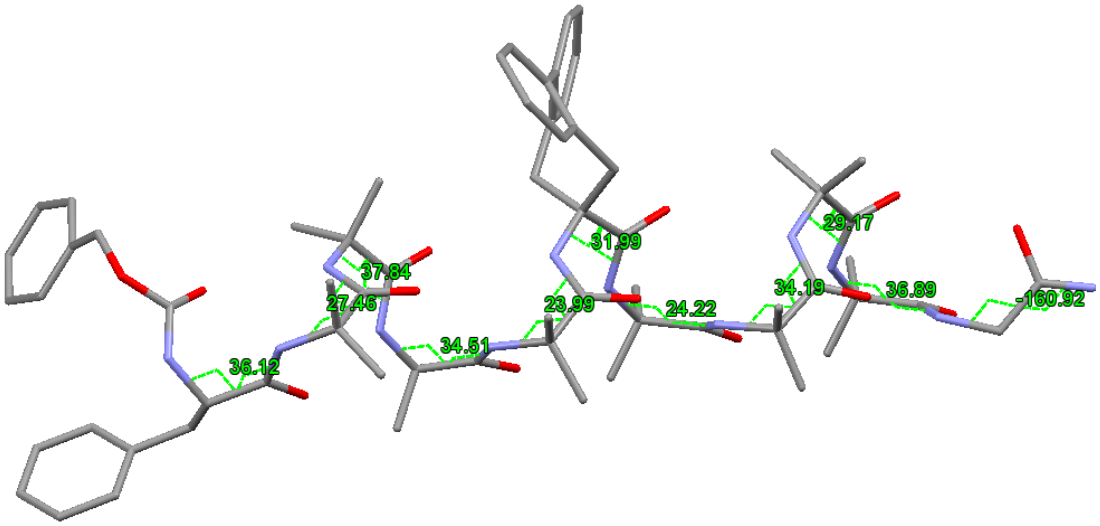

Figure S65. Highlighting the ϕ torsion angles for one molecule in the unit cell for Cbz-L-Phe-$(Aib)_4$-Bip-$(Aib)_4$-$GlyNH_2$.

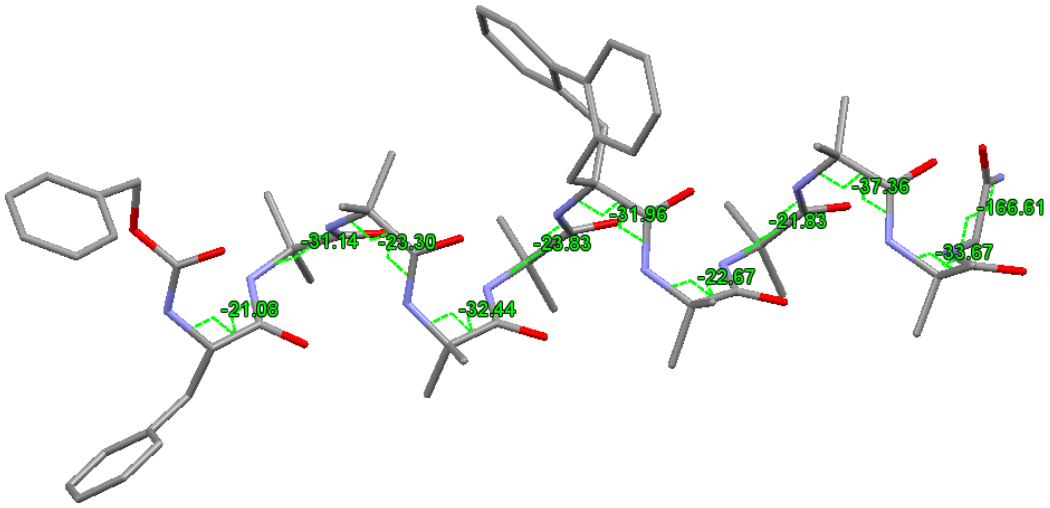

Figure S66. Highlighting the ϕ torsion angles for one molecule in the unit cell for Cbz-L-Phe-$(Aib)_4$-Bip-$(Aib)_4$-$GlyNH_2$.

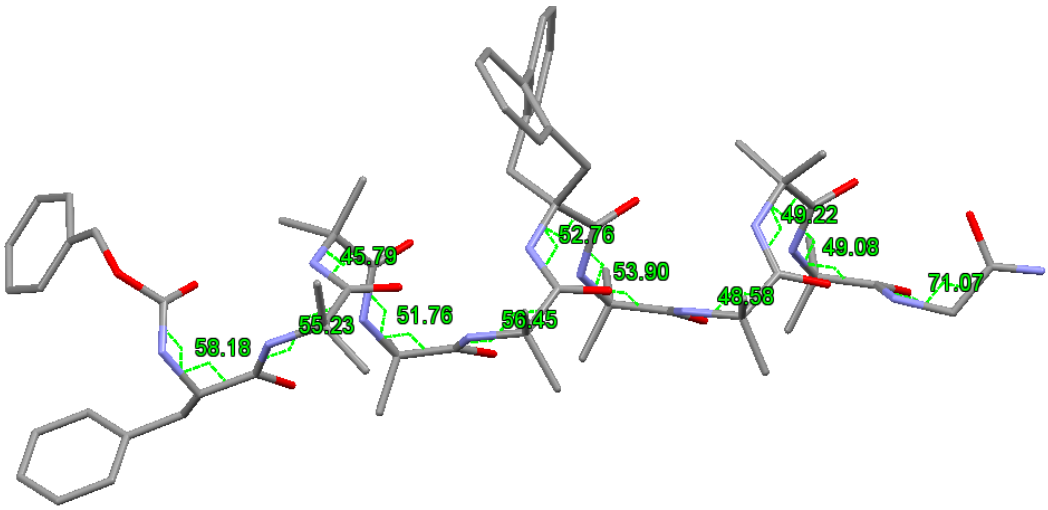

Figure S67. Highlighting the Ψ torsion angles for one molecule in the unit cell for Cbz-L-Phe-$(Aib)_4$-Bip-$(Aib)_4$-$GlyNH_2$.

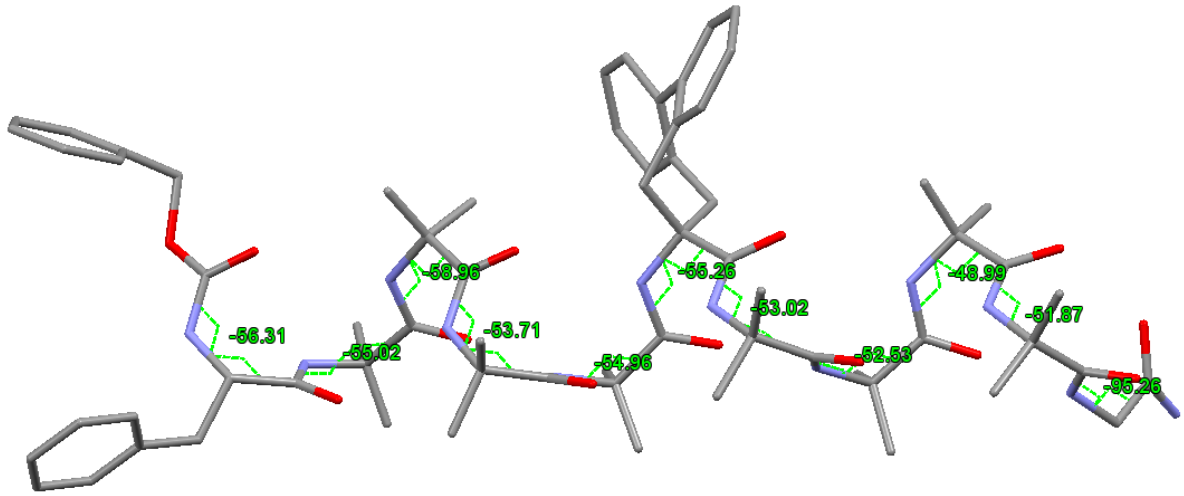

Figure S68. Highlighting the Ψ torsion angles for one molecule in the unit cell for Cbz-L-Phe-$(Aib)_4$-Bip-$(Aib)_4$-$GlyNH_2$.

Intramolecular Hydrogen-bonding interactions in Cbz-L-Phe-$(Aib)_4$-Bip-$(Aib)_4$-$GlyNH_2$.

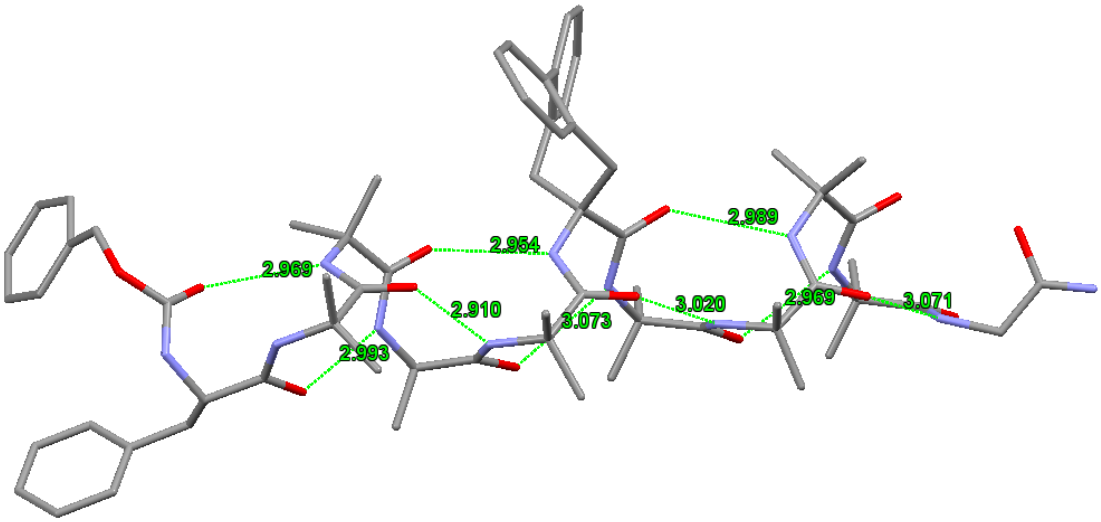

Figure S69. Intramolecular hydrogen bonding interactions present in one molecule of Cbz-L-Phe-$(Aib)_4$-Bip-$(Aib)_4$-$GlyNH_2$found in the unit cell.

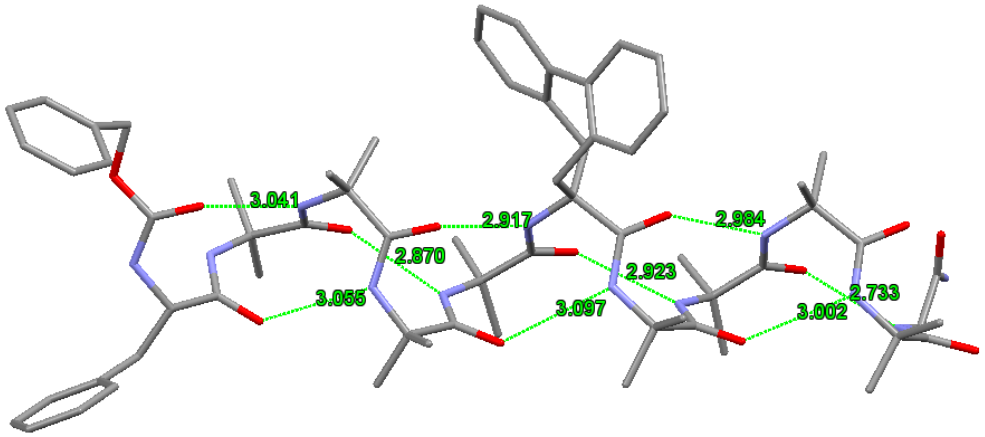

Figure S70. Intramolecular hydrogen bonding interactions present in one molecule of Cbz-L-Phe-$(Aib)_4$-Bip-$(Aib)_4$-$GlyNH_2$ found in the unit cell.

Packing of Cbz-L-Phe-$(Aib)_4$-Bip-$(Aib)_4$-$GlyNH_2$ in the unit cell

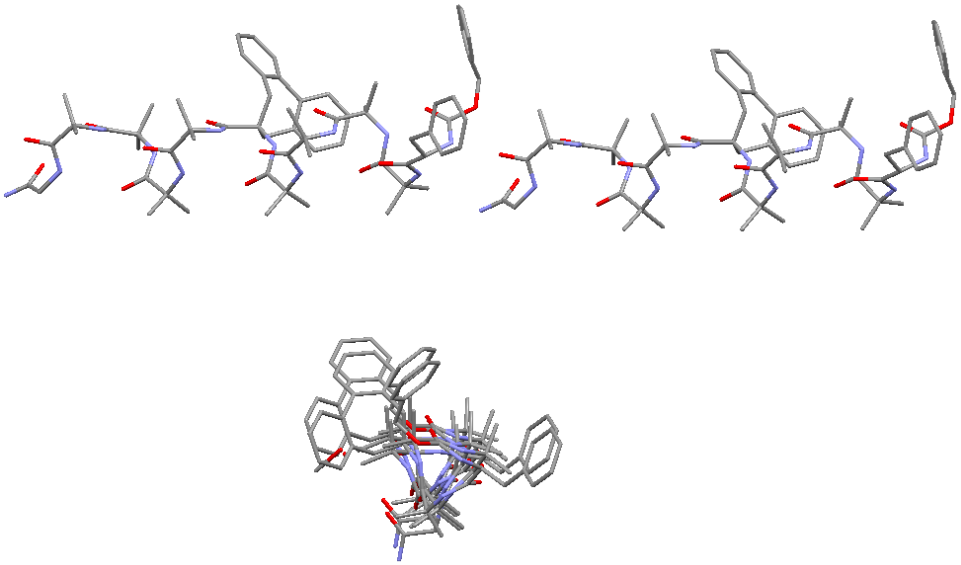

Figure S71. Packing of molecules in the unit cell of Cbz-L-Phe-$(Aib)_4$-Bip-$(Aib)_4$-$GlyNH_2$.

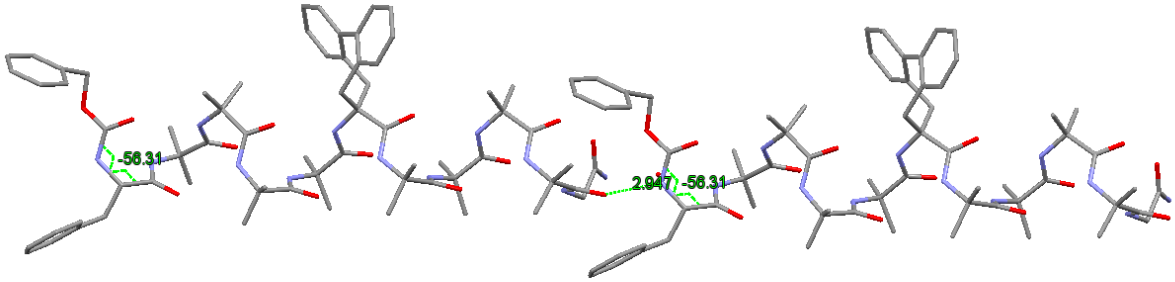

Figure S72. Intermolecular hydrogen bonding interaction present between two molecules of Cbz-L-Phe-$(Aib)_4$-Bip-$(Aib)_4$-$GlyNH_2$ of the same screw-sense preference found in the unit cell.

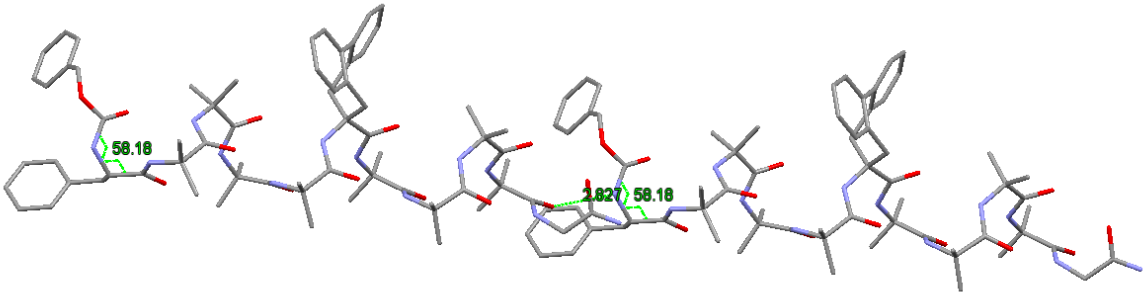

Figure S73. Intermolecular hydrogen bonding interaction present between two molecules of Cbz-L-Phe-$(Aib)_4$-Bip-$(Aib)_4$-$GlyNH_2$ of the same screw-sense preference found in the unit cell.

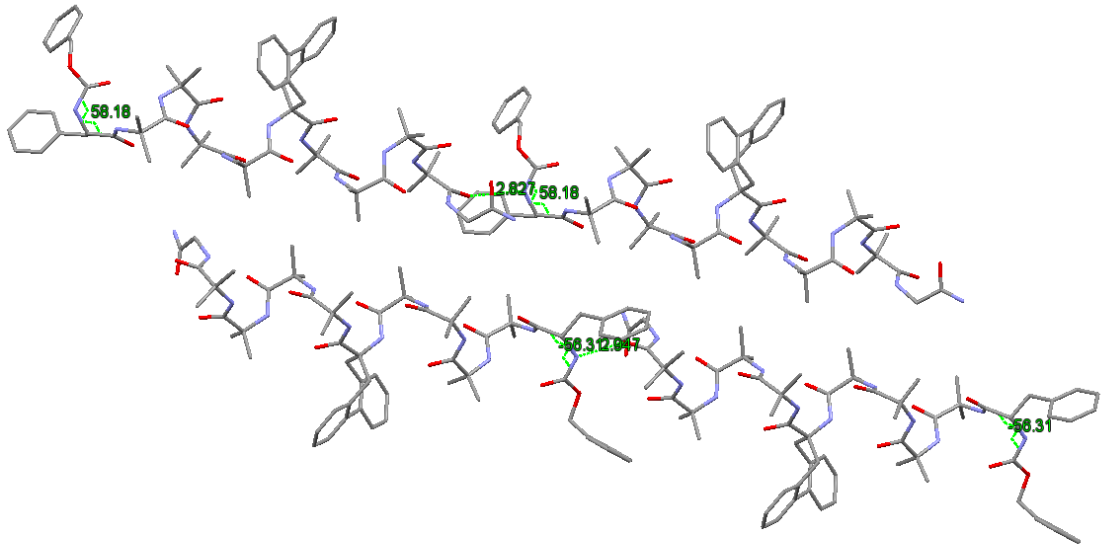

Figure S74. Packing of Cbz-L-Phe-$(Aib)_4$-Bip-$(Aib)_4$-$GlyNH_2$ in the unit cell with pseudo-symmetry with a non-crystallographic C_2 axis.

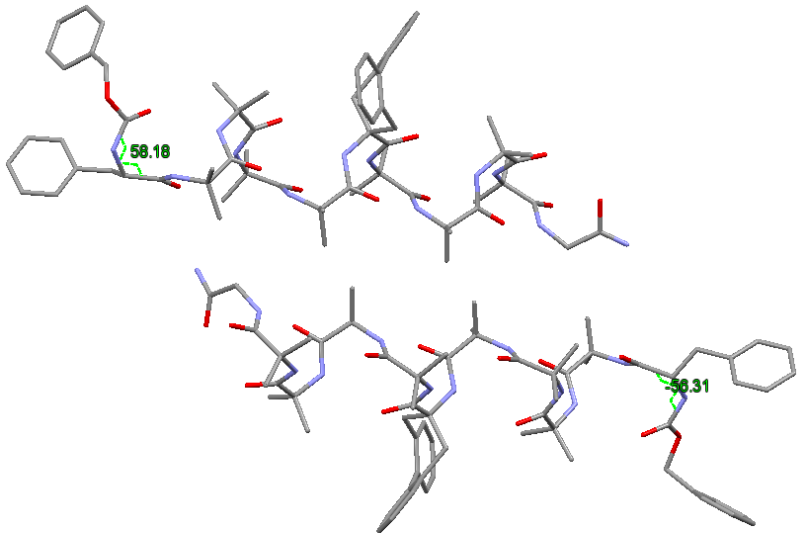

Figure S75. Packing of Cbz-L-Phe-$(Aib)_4$-Bip-$(Aib)_4$-$GlyNH_2$ in the unit cell with pseudo-symmetry with a non-crystallographic C_2 axis.

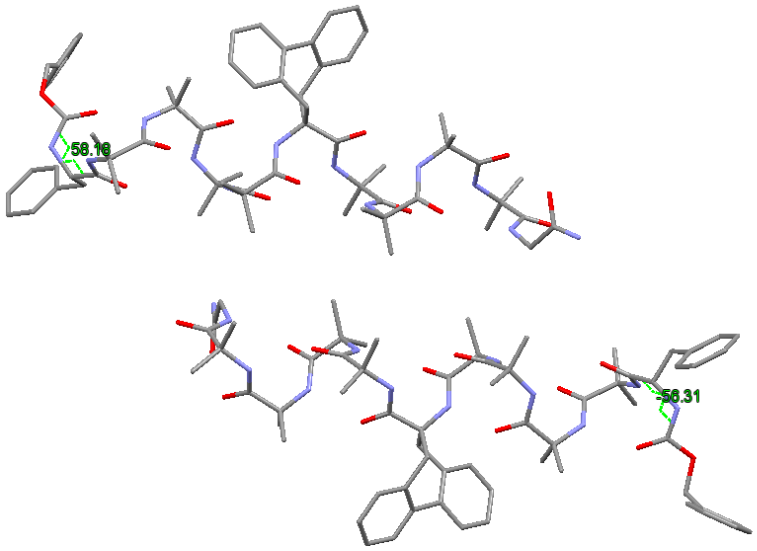

Figure S76. Packing of Cbz-L-Phe-$(Aib)_4$-Bip-$(Aib)_4$-$GlyNH_2$ in the unit cell with pseudo-symmetry with a non-crystallographic C_2 axis.

Length of 3_{10} Helical Conformation in Cbz-L-Phe-$(Aib)_4$-Bip-$(Aib)_4$-$GlyNH_2$

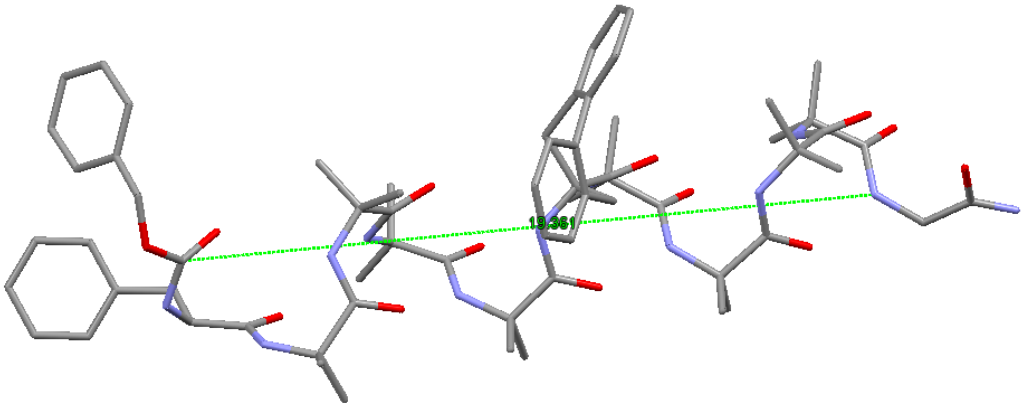

Figure S77. Length of 3_{10} helical conformation adopted by Cbz-L-Phe-$(Aib)_4$-Bip-$(Aib)_4$-$GlyNH_2$for one molecule in the unit cell.

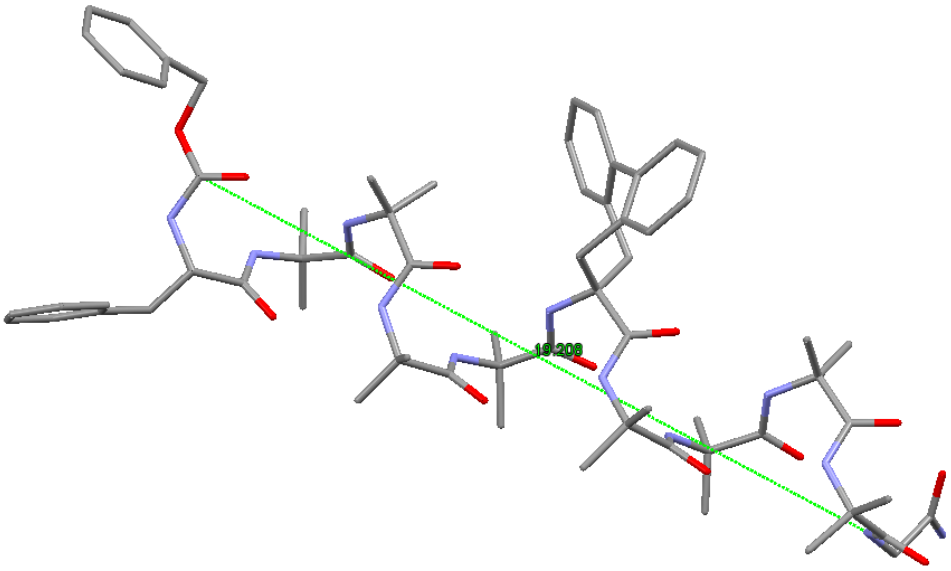

Figure S78. Length of 3_{10} helical conformation adopted by Cbz-L-Phe-$(Aib)_4$-Bip-$(Aib)_4$-$GlyNH_2$for one molecule in the unit cell.

Axial Chirality in Bip Residue in Cbz-L-Phe-$(Aib)_4$-Ac_5c-$(Aib)_4$-$GlyNH_2$

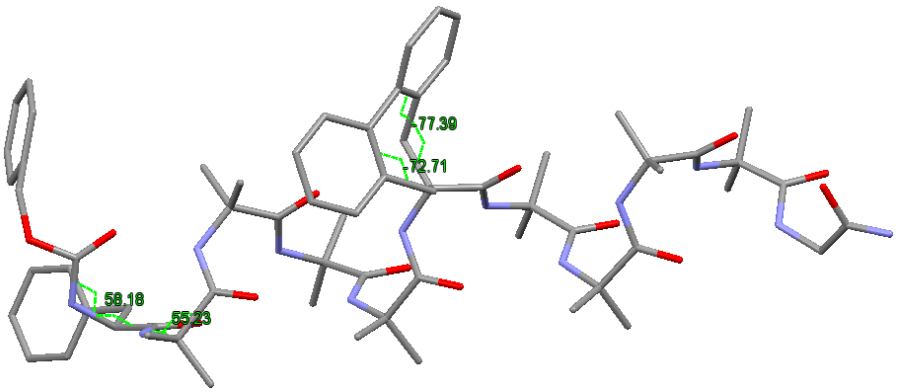

Figure S79. Axial chirality of Bip residue in the *P* helix of Cbz-L-Phe-$(Aib)_4$-Bip-$(Aib)_4$-$GlyNH_2$.

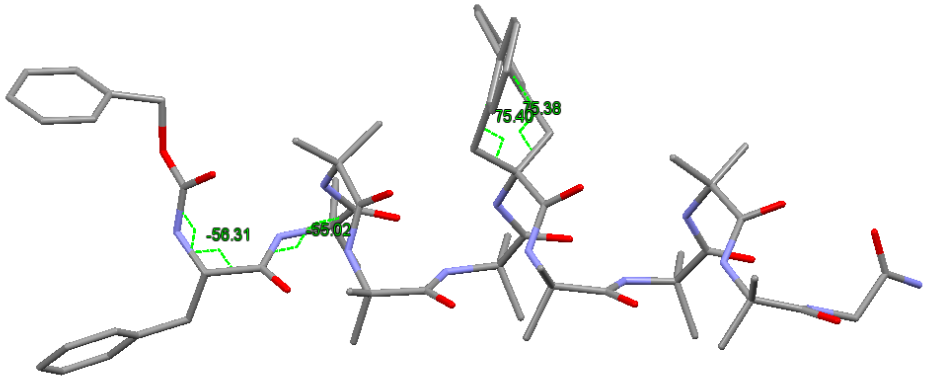

Figure S80. Axial chirality of Bip residue in the *M* helix of Cbz-L-Phe-$(Aib)_4$-Bip-$(Aib)_4$-$GlyNH_2$.

Appendix: ^{1}H, ^{13}C NMR spectra

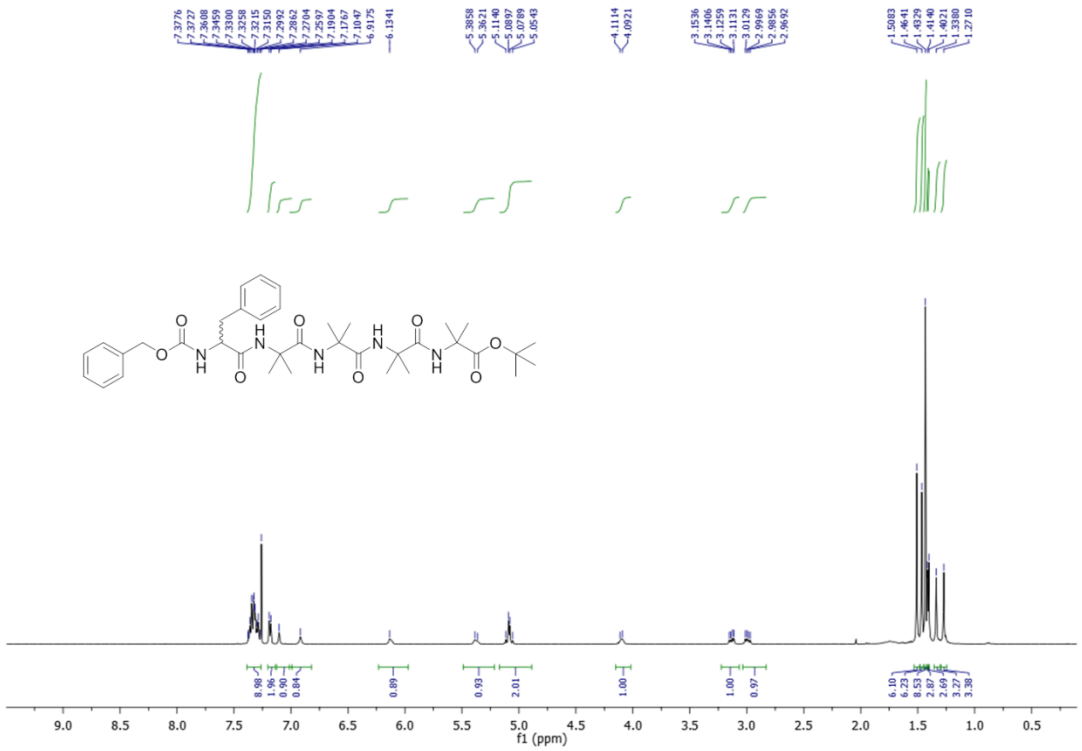

^{1}H NMR spectrum (500 MHz, $CDCl_3$) of CbzPheAib$_4$O^{t}Bu.

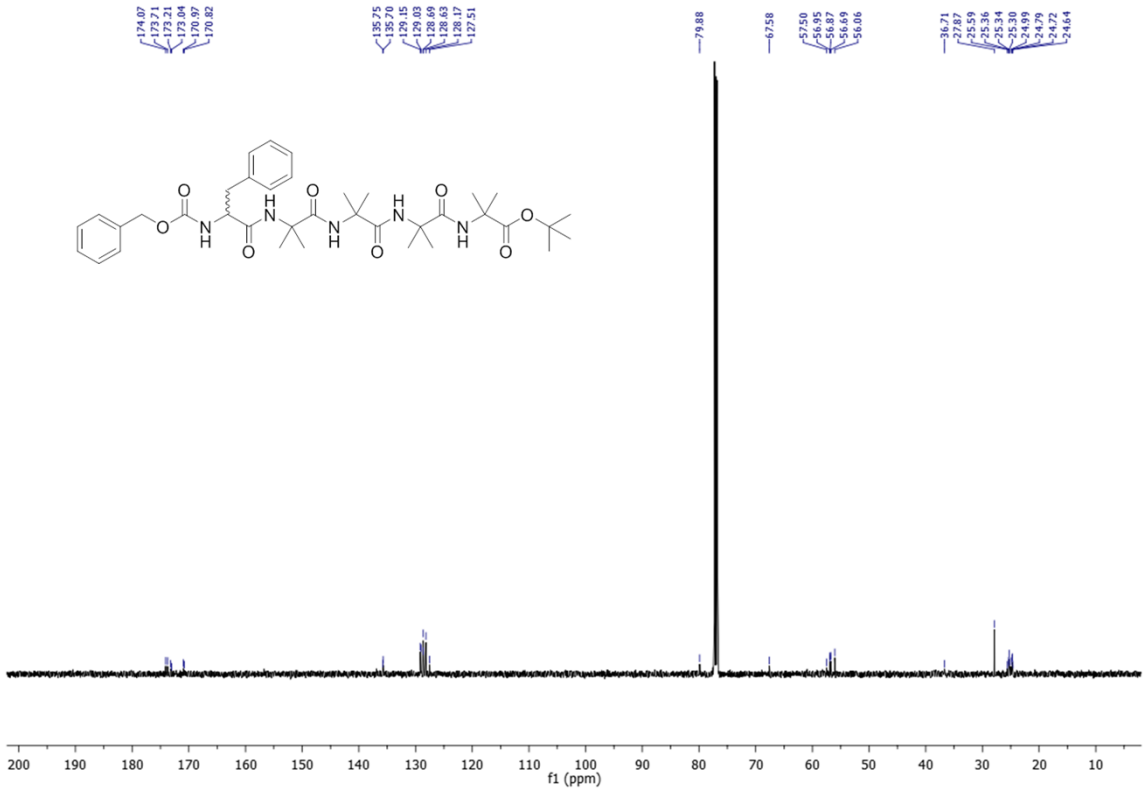

^{13}C NMR spectrum (125 MHz, $CDCl_3$) of CbzPheAib$_4$O^{t}Bu.

References

1. J. Clayden, A. Castellanos, J. Solà, G. A. Morris, *Angew. Chem. Int. Ed.,* **2009**, *48*, 5962.

2. L. Byrne, J. Solà, T. Boddaert, T. Marcelli, R. W. Adams, G. A. Morris, J. Clayden, *Angew. Chem. Int. Ed.,* **2014**, *53*, 151.